Partial Differential Equations and Applications (2022) 3:75
https://doi.org/10.1007/s42985-022-00214-y

ORIGINAL PAPER

Finite element approximation of invariant manifolds by the parameterization method

Jorge Gonzalez[1] · J. D. Mireles James[2] · Necibe Tuncer[2]

Received: 6 January 2022 / Accepted: 2 October 2022

Abstract
We combine the parameterization method for invariant manifolds with the finite element method for elliptic PDEs, to obtain a new computational framework for high order approximation of invariant manifolds attached to unstable equilibrium solutions of nonlinear parabolic PDEs. The parameterization method provides an infinitesimal invariance equation for the invariant manifold, which we solve via a power series ansatz. A power matching argument leads to a recursive systems of linear elliptic PDEs—the so called homological equations—whose solutions are the power series coefficients of the parameterization. The homological equations are solved recursively to any desired order N using finite element approximation. The end result is an N-th order polynomial approximation of a chart map of the manifold, with coefficients in an appropriate finite element space. We implement the method for a variety of example problems having both polynomial and non-polynomial nonlinearities, on non-convex two dimensional polygonal domains (not necessary simply connected), for equilibrium solutions with Morse indices one and two. We implement a-posteriori error indicators which provide numerical evidence in support of the claim that the manifolds are computed accurately.

Keywords Parabolic partial differential equations · Unstable manifold · Finite element analysis · Formal Taylor series

Submitted to the editors DATE.

This article is part of the section "Computational Approaches" edited by Siddhartha Mishra.

✉ J. D. Mireles James
jmirelesjames@fau.edu
http://www.math.fau.edu/people/faculty/mirelesjames.php

Jorge Gonzalez
jgonzalez35@gatech.edu
https://people.math.gatech.edu/ jgonzalez35/index.html

Necibe Tuncer
ntuncer@fau.edu
http://www.math.fau.edu/people/faculty/tuncer.php

[1] School of Mathematics, Georgia Institute of Technology, Atlanta, GA, USA

[2] Department of Mathematical Sciences, Florida Atlantic University, Boca Raton, FL, USA

Published online: 21 October 2022

Mathematics Subject Classification 68Q25 · 68R10 · 68U05

1 Introduction

The present work concerns nonlinear stability analysis for parabolic partial differential equations (PDEs). In particular, we develop high order numerical methods for approximating local unstable manifolds attached to equilibrium solutions of finite Morse index (finite number of unstable eigenvalues counted with multiplicity) for parabolic PDEs formulated on spatial domains with non-trivial geometry. We show that the Taylor coefficients of an appropriate parameterization of the local unstable manifold solve a *homological equation* which is strongly related to the eigenvalue problem/resolvent of the linearization at equilibrium. Our main goal is to leverage this result in the development of efficient numerical algorithms. We stress that, since we compute the Taylor coefficients order by order by directly solving the homological equations, our method does not require numerical integration of the parabolic PDE.

Recall that the equilibrium solutions of a parabolic PDE are found by solving the steady state equation, and that this equation usually reduces to an elliptic BVP. Likewise, the eigenvalue problems which determine the linear stability of an equilibrium solution are linear elliptic BVPs of the same kind. Because of this, there are dramatic differences between parabolic problems in the case of one spatial variable and in the case of two or more. For problems with one spatial variable, equilibrium and eigenvalue problems lead to two point BVPs for ordinary differential equations (ODEs). Such problems are generally amenable to spectral methods (Fourier series) which diagonalize both differential operators and multiplication (in Fourier and function space respectively) and which typically have excellent convergence properties. Parabolic PDEs in two or more spatial variables posed on domains with non-trivial geometry require fundamentally different theoretical and numerical tools. Finite element analysis is invaluable in this context, and—since finite element methods typically employ lower regularity approximation schemes—it is often necessary to study a weak formulation of the BVP.

Our approach is rooted in the tradition of the qualitative theory of dynamical systems, and exploits the parameterization method of Cabré, Fontich, and de la Llave [10–12]. The idea of the parameterization method is to study an auxiliary functional equation, whose solutions correspond to chart maps of the invariant object. The method is used widely in the field of computational dynamics. The basic mathematical setup and some additional references are discussed in Sect. 2.1. We extend the parameterization method to parabolic PDEs on non-trivial domains, and illustrate it's utility by implementing numerical computations for a number of example systems.

- **The Fisher Equation:** scalar reaction/diffusion equation with logistic nonlinearity. This pedagogical example illustrates the main steps of our procedure in the easiest possible setting.
- **The Ricker Equation:** a modification of the Fisher equation with a more realistic exponential nonlinearity. We show how non-polynomial problems are treated using ideas from automatic differentiation for formal power series.
- **A modified Kuramoto-Shivisinsky Equation:** a scalar parabolic PDEs with the biharmonic Laplacian as the leading term and lower order derivatives in the nonlinearities. The system is a toy model of fluid dynamics.

For each example we derive the homological equations, and implement numerical procedures for solving them. In the case of a non-polynomial nonlinearity, the necessary formal series manipulations are simplified by coupling the given PDEs to auxiliary equations describing the transcendental nonlinear terms. We provide examples of this procedure, and develop power series expansions for unstable manifolds attached to equilibria with Morse indices 1 and 2. This provides examples of computations for one and two dimensional unstable manifolds. The Fisher and Ricker Equations are nonlinear heat equations, and we use piecewise linear finite elements to approximate the coefficients of the parameterization. Kuramoto-Shivisinsky is a bi-harmonic Laplacian equation, so that higher order elements are appropriate. Here we utilize the Argyris element. We implement a-posteriori error indicators for each of the examples, giving evidence that the manifolds have been computed correctly.

Remark 1.1 (Invariant manifolds for 1D domains) We remark that Fourier-Taylor methods for computing invariant manifolds for parabolic problems in one spatial dimension are treated in a number of places, for example in [2, 38, 54], and higher dimensional problems with periodic boundary conditions (including Dirchlet/Neumann boundary conditions on rectangles/boxes) can also be studied using multivariate Fourier series. We refer to the works of [7, 8, 14, 23, 35] for more discussion of invariant manifolds in this context.

The remainder of the paper is organized as follows. In Sect. 2 we review the finite element method for elliptic PDEs, and the parameterization method for invariant manifolds on Hilbert spaces. We also provide an elementary example of the formal series analysis for the unstable manifold in a simple finite dimensional example. In Sect. 3 we extend the parameterization method to a class of parabolic problems. Section 4 contains the main calculations of the paper, as we derive the homological equations for the main examples. We also implement the recursive solution of the homological equations for the main examples and report on some numerical results. Some conclusions and reflections are found in Sect. 5.

2 Background

While the material in this section is standard in some circles, the methods of the present work combine tools from different fields and it is worth reviewing some basic ideas. Our hope is that some brief review will help to make the paper more self contained. The reader familiar with these ideas may want to skip ahead to Sect. 3, and refer back to these sections only as needed.

2.1 The parameterization method

The parameterization method is a general functional analytic framework for studying invariant manifolds, originally developed for fixed points for maps on Banach spaces [10–12], and for whiskered tori of quasi-periodic maps [25–27]. Since then it has been extended to a number of settings for both discrete and continuous dynamical systems, in both finite and infinite dimensions. A complete overview of the literature is beyond the scope of the present brief introduction, and the interested reader will find a much more complete overview—including a wealth of references to the literature—in the recent book on the topic [24]. Several papers more closely related to the present work include works of [22, 28, 29] on delay differential equations, KAM for PDEs [17], and unstable manifolds for PDEs defined on compact intervals [38], and on the whole line [2]. More recently the parameterization method has been

used to develop a mathematically rigorous approach to optimal mode selection in nonlinear model reduction by projecting onto spectral submanifolds [6, 9, 33]. This research direction has been further developed and combined with large finite element systems demonstrating its potential for industrial applications [48, 56].

2.1.1 Parameterization method for vector fields on Hilbert spaces

We give a brief review the parameterization method, in the context of evolution problems on Hilbert spaces. The main application we have in mind is the dynamics of a semi-flow generated by parabolic PDE. In particular, we discuss the invariance equation for the local unstable manifold attached to an equilibrium solution.

Let $\mathcal{H}$ be an L^2 Hilbert space (H^k or H_0^k for some k) and $F\colon \mathcal{H} \to L^2$ be a Frechet differentiable mapping. We adopt also the standard requirement that $DF(x)$, when viewed as an operator on L^2, is densely defined and sectorial. Consider the evolution equation

$$\frac{\partial}{\partial t}u(t) = F(u(t)), \qquad \text{with } u(0) \in \mathcal{H} \text{ given.} \tag{2.1}$$

An orbit segment (or *solution curve*) for Eq. (2.1) is a smooth curve $\gamma\colon (a, b) \to \mathcal{H}$ having

$$\frac{d}{dt}\gamma(t) = F(\gamma(t)),$$

for each $t \in (a, b)$. If $b = \infty$ then γ is a said to be a full forward orbit. Since F dose not depend on time, we can always choose $a = 0$.

The simplest type of orbits are equilibria, that is, solutions which do not change in time. For $u_0 \in \mathcal{H}$, the curve $\gamma(t) = u_0$ is a constant solution of Eq. (2.1) if and only if

$$F(u_0) = 0.$$

For a given equilibrium solution u_0, we would like to understand first it's linear stability, and then it's nonlinear stability. That is, we would like to understand how orbits in a neighborhood of u_0 escape from that neighborhood.

Let $A = DF(u_0)$, and define the Morse index of u_0 to be the number of unstable eigenvalues of A, counted with multiplicity. We assume that Eq. (2.1) is parabolic, so that A generates a compact semi-group e^{At}. This insures that the Morse index of A is finite. Let $\lambda_1, \ldots, \lambda_M$ denote the unstable eigenvalues ordered so that

$$0 < \text{real}\,(\lambda_1) \le \cdots \le \text{real}\,(\lambda_M)\,.$$

Suppose for the sake of simplicity that each unstable eigenvalue has multiplicity one, and that they are all real (though both assumptions can be removed—see [10, 55]), and let $\xi_1, \ldots, \xi_M \in \mathcal{H}$ denote associated eigenfunctions, so that

$$A\xi_j = \lambda_j \xi_j, \qquad 1 \le j \le M.$$

Suppose that $\gamma\colon (-\infty, 0] \to \mathcal{H}$ is a solution curve for Eq. (2.1) and that $u \in \mathcal{H}$. We say that γ is an infinite pre-history for u, accumulating in backward time to the equilibrium u_0, if

$$\gamma(0) = u, \qquad \text{and} \qquad \lim_{t\to-\infty} \gamma(t) = u_0.$$

The unstable manifold attached to u_0, denoted $W^u(u_0)$, is the set of all $u \in \mathcal{H}$ which have an infinite pre-history, accumulating at u_0. The intersection of $W^u(u_0)$ with a neighborhood

U of u_0 is called a local unstable manifold for u_0, and is denoted by

$$W^u(u_0) \cap U = W^u_{\text{loc}}(u_0, U).$$

By the unstable manifold theorem, there exists a neighborhood U of u_0 so that $W^u_{\text{loc}}(u_0, U)$ is a smooth manifold, diffeomorphic to an M-disk, and tangent to the unstable eigenspace of A at u_0. Moreover, if A is hyperbolic (that is, if A has no eigenvalues on the imaginary axis), then $W^u_{\text{loc}}(u_0, U)$ is the set of all $u \in U$ which have well-defined backwards history remaining in a neighborhood of u_0 for all time $t \leq 0$.

We are now ready to introduce the parameterization method. Let $\mathbb{B} = [-1, 1]^M$ denote the M-dimensional unit hypercube. We seek a

$P : \mathbb{B} \to \mathcal{H}$ having that

$$P(0) = u_0, \tag{2.2}$$

$$\partial_j P(0) = \xi_j, \qquad 1 \leq j \leq M, \tag{2.3}$$

and that

$$P\left([-1, 1]^M\right) \subset W^u_{\text{loc}}(u_0, U),$$

for some open set U containing u_0. Any such P is a local unstable manifold attached to u_0. Since any reparameterization of P is again a parameterization of a local unstable manifold, the problem has infinitely many freedoms and we need to impose an additional (infinite dimensional) constraint to isolate a single parameterization.

Write

$$\Lambda = \begin{pmatrix} \lambda_1 & \dots & 0 \\ \vdots & \ddots & \vdots \\ 0 & \dots & \lambda_M \end{pmatrix}. \tag{2.4}$$

The main idea of the parameterization method is to look for P which, in addition to satisfying the constraint Eqs. (2.2) and (2.3), is a solution of the *invariance equation*

$$F(P(\theta)) = DP(\theta)\Lambda\theta, \qquad \text{for all } \theta \in \mathbb{B} = [-1, 1]^M. \tag{2.5}$$

We remark that the choice of "unit" domain is a normalization which will become more clear as we proceed.

Figure 1 illustrates the geometric meaning of Eq. (2.5). The equation requires that the push forward of the linear vector field Λ by DP equals the vector field F restricted to the image of P. Loosely speaking, since the two vector fields match on the image of P they must generate the same dynamics—with the dynamics generated by Λ well understood. We then

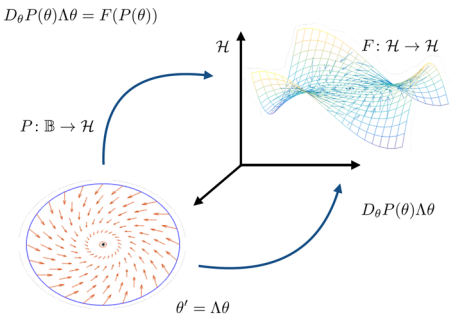

Fig. 1 Schematic representation of the invariance equation given in Eq. (2.5). The idea is the DP pushes forward the vector field Λ modeling the dynamics on the unstable manifold. This push forward should be equal, on the image of P, to the vector field F generating the full dynamics

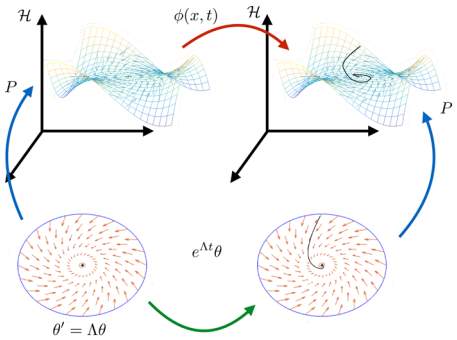

Fig. 2 The orbit correspondence induced by the invariance Equation. The orbits generated by the vector field Λ accumulate in backwards time to the origin in $\mathbb{B}$. Then P lifts these orbits to orbits in $\mathcal{H}$ which accumulate at the equilibrium u_0. From this it follows that image of P is a local unstable manifold. or (2.5)

expect that P maps orbits of Λ in $\mathbb{B}$ to orbits of F on the image of P. Since P maps orbits to orbits, Eq. (2.5) is called an infinitesimal conjugacy equation. The geometric meaning of Eq. (2.5) is illustrated in Fig. 2, and is made precise by the following lemma, whose proof appears in Appendix C

Lemma 2.1 (Orbit correspondence) *Assume that the unstable eigenvalues $\lambda_1, \ldots, \lambda_M$ are real and distinct. Suppose that $P : [-1, 1]^M \to \mathcal{H}$ satisfies the first order constraints of Eqs. (2.2) and (2.3), and that P is a smooth solution of Eq. (2.5) on $\mathbb{B} = (-1, 1)^M$. Then P parameterizes a local unstable manifold for u_0.*

We remark that if F generates a semi-flow Φ near u_0, then Lemma 2.1 says that P satisfies the flow conjugacy

$$P(e^{\Lambda t}\theta) = \Phi(P(\theta), t), \tag{2.6}$$

for all t such that $e^{\Lambda t}\theta \in (-1, 1)^M$. That is, P conjugates the flow generated by Λ to the flow generated by F.

An example illustrating the formal series solution of Eq. 2.5 for a simple ODE is given in Appendix A, with some numerical calculations given in Appendix B. These appendices are included for the reader who would like to see how the method works in the simplest possible setting before moving on to the more sophisticated applications to PDEs considered in the next section, in hopes of making the present work self contained. Other similar worked examples are found in the literature, and we refer the interested reader to [4, 13, 21, 53] for more details.

Remark 2.2 *(Complex conjugate unstable eigenvalues)* Complex conjugate eigenvalues are easily incorporated into this set-up by choosing associated complex conjugate eigenfunctions and proceeding as above. This results in complex conjugate coefficients for the parameterization P. The use of complex conjugate variables (in the appropriate components of θ) results in P having real image, i.e. recovers the parameterization of the real manifold. The only difference is that one has to adjust the domain of the parameterization in the variables corresponding to the complex conjugate eigenvalues, choosing unit disks instead of unit intervals. In this sense the PDE case is no different from the ODE case described in detail in [36], where the interested reader can find more a complete discussion.

2.2 Finite element methods for elliptic linear elliptic PDE

In this section we briefly review some basic finite element analysis for elliptic BVPs needed for our numerical implementations. Excellent reference for this now classic material include

[16, 19]. Let $\Omega \subset \mathbb{R}^d$ denote an open set and let $\mathcal{H}$ be an L^2 Sobolev space on Ω (and hence a Hilbert space). Let $\mathcal{H}^\vee$ denote the dual space consisting of all bounded linear functionals on $\mathcal{H}$.

Consider for example a uniformly elliptic linear PDE of the form

$$\mathcal{L}u = f,$$

with Dirichlet boundary conditions $u|_{\partial\Omega} = 0$. We ask that $\mathcal{L}$ is densely defined on $\mathcal{H} \subset L^2$, and that $f \in L^2$.

A weak formulation of the problem is obtained after multiplying by a test-function $v \in \mathcal{H}$, applying Green's formula (integration by parts), and imposing the boundary conditions. This results in the variational problem

$$\text{Find} \quad u \in \mathcal{H} \quad \text{such that} \quad \forall v \in \mathcal{H}, \quad \langle u, v\rangle_{\mathcal{L}} = \langle f, v\rangle, \tag{2.7}$$

where

$$\langle f, v\rangle = \int_\Omega fv,$$

and $\langle u, v\rangle_{\mathcal{L}}$ is a bilinear form. More generally, one can ask that $\mathcal{L}\colon \mathcal{H} \to \mathcal{H}^\vee$ and that $f \in \mathcal{H}^\vee$, where $\vee$ denotes the dual space.

The classical *Lax-Milgram lemma* insures that the problem has a unique solution u, assuming that $\langle\cdot,\cdot\rangle_{\mathcal{L}}\colon \mathcal{H} \times \mathcal{H} \to \mathbb{R}$ is a continuous $\mathcal{H}$-elliptic bilinear form and $\langle f, \cdot\rangle\colon \mathcal{H} \to \mathbb{R}$ is a bounded linear functional (i.e, $\langle f, \cdot\rangle \in \mathcal{H}^\vee$). Neumann boundary conditions are handled using the same technology, after restricting to a space $\mathcal{H}$ of test functions which vanish on $\partial\Omega$. The treatment of more general boundary conditions using penalty methods, Lagrange multipliers, or projection methods is also classical. We refer to [1, 3, 15, 20, 52] for more general discussion of boundary conditions.

The finite element method (FEM) is a Galerkin projection approach to numerically solving Eq. (2.7), and consists of three main steps:

1. Triangulate $\Omega \subset \mathbb{R}^d$: obtain (often polygonal) mesh which discretizes the problem domain.
2. Choose interpolants for $\mathcal{H}$ on the mesh: construct a basis for the interpolant space where the basis functions have nearly disjoint support over mesh elements. This is the finite element basis and its span is a finite element space.
3. Solve the sparse linear system obtained by projecting the the weak formulation of the PDE (Eq. (2.7)) onto the finite element basis. This reduces the problem to numerical linear algebra.

In the present work we focus on $\Omega \subset \mathbb{R}^2$ a polygonal domain. However, we do not require Ω to be convex or even simply connected, and use the domains illustrated in Fig. 3. The next three subsections discuss the three steps listed above in more detail.

2.2.1 Triangulation of $\Omega \subset \mathbb{R}^2$

Let $\{T_i\}_{i=1}^{ne}$ denote the elements of the triangulation so that

$$\Omega = \bigcup_{i=1}^{ne} T_i.$$

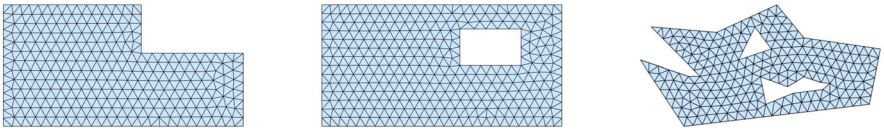

Fig. 3 Three example domains used in this paper. Note that they are non-convex, and non-simply connected. Left: the L domain: it has a reemergent corner. Center: the *Door* domain: not simply connected. Right: the *Polygon with holes* domain: toy model of a "natural" domain like a lake with islands

Here T_i is the i^{th} triangle, and ne is the number of triangles. We require that if the boundary of two triangles meet, then their intersection must be at a common edge. We remark that other discretizations can be considered, for example as in the Bogner-Fox-Schmit elements [16] (quadrilaterals), or even a combination of rectangles and triangles. Also, the discretization does not need to be uniform but can be adapted to the model and domain, leading to more efficient approximations.

2.2.2 Constructing the basis elements

The basis elements, which are required to have "small" compact support in $\mathcal{H}$, are typically chosen to be piecewise polynomial. In this paper we use linear polynomials for second order problems (Laplacian operator), and fifth degree polynomials for some fourth order examples (Bi-harmonic Laplacian). These Argyris elements are discussed in more detail in Sect. 4.4. More general basis elements can be considered such as special rational functions (for example Zienkiewicz triangles [16]).

A finite element is denoted by $E = [z_1, \ldots, z_{nn}] \subset T$, where T is an arbitrary triangle and the z_i are *control points* or *nodes*. $S_i := \{L_{ij} : 1 \leq j \leq s_i\}$ denotes a corresponding sets of *control operators* evaluated at z_i (nn is the number of nodes in T and s_i denotes the total number of operators assigned to the node z_i). Typically, the nodes consist of the vertices along with a few other carefully chosen points. In general, they are not required to be uniformly distributed in T.

Denote by $lnb := \sum_{k=1}^{nn} s_k$ and define

$$S = \bigcup_{i=1}^{nn} S_i = \{L_i : 1 \leq i \leq lnb\}.$$

the set of operators associated with the finite element E. The letters lnb appropriately stand for "local number of basis" since the operators are used to determine the basis elements associated with T. That is, for each k, the system $L(\phi) := (L_1(\phi), \cdots, L_{lnb}(\phi)) = e_k$ is required to have a unique solution ϕ_k^E in some vector space $\mathcal{B} \subset \mathcal{H}$. Here e_k is the k^{th} elementary basis vector in $\mathbb{R}^{lnb}$.

It follows that if we would like to work with

$$\mathcal{B} = \mathbb{P}_k := \{p : p \text{ is a polynomial of degree at most } k\},$$

then we must have $lnb = \frac{(k+1)(k+2)}{2}$. Imposing regularity conditions (for example continunity) on the solution u imposes further restrictions on the finite elements. For $\mathcal{B} = \mathbb{P}_1$ the elements are of the form $E = [n_1, n_2, n_3]$ where the n_i's are the vertices of the triangles, and $S_i = \{id\}$ for all i's, with $id(\phi)(n_i) = \phi(n_i)$.

Finally, let $V_h := \text{span}\{\phi_i\}_{i=1}^{nb} \subset \mathcal{H}$ denote an interpolation space for $\mathcal{H}$, where nb is the total number of basis elements. Constructing this space involves collecting and indexing all the local basis functions.

2.2.3 Computing the projection

Let $u \in \mathcal{H}$ denote the solution of Eq. (2.7). The projection of u into V_h is found by solving a weak formulation of Eq. (2.7) on V_h. More precisely, write $u_h = \sum_{i=1}^{nb} c_i \phi_i$ and solve the linear system

$$\sum_{j=1}^{nb} c_j \langle \phi_j, \phi_i \rangle_{\mathcal{L}} = \langle f, \phi_i \rangle. \tag{2.8}$$

It follows that the matrix $\left(\langle \phi_j, \phi_i \rangle_{\mathcal{L}}\right)$ is invertible under the assumption that $\langle ., . \rangle_{\mathcal{L}}$ is $\mathcal{H}$-elliptic and the ϕ_i are linearly independent.

In general, a Lagrange type interpolation of a function f over T with control set $\{S_i\}$ is given by

$$\Pi_T(f)(x, y) = \sum_{i=1}^{lnb} L_i(f)(z_{n(i)}) \frac{det(A_i(x, y))}{det(A)}$$

where $L_i \in S = \bigcup_{i=1}^{nn} S_i$, and the index $n(i) = k$ for i such that $s_0 + \cdots s_{k-1} + 1 \leq i \leq s_0 + \cdots s_k$. Here we define $A_{ij} = \left(L_i(x^m y^n)(z_{n(i)})\right)$, and $(A_k(x, y))_{ij} = (1 - \delta_{ki})A_{ij} + \delta_{ki} x^m y^n$, where $j = \frac{(m+n)(m+n+1)}{2} + (n + 1)$. The operators L_i are acting on the monomials $x^m y^n$ where m, n range from 0 to the order of the polynomial interpolation, and the the coordinate j depends on m, n as described above. Notice that the only term that survives the evaluation of $L_i(\Pi_T(f))$ at a node gives the prescribed value. We let $S_0 := \emptyset$ for convenience of expressing $n(i)$.

For low order polynomial bases the integrals appearing in (2.8) can be evaluated exactly. For higher order bases it is often more practical to use quadrature rules of sufficiently high degree to approximate the integrals. Such rules have the form

$$\int_\Omega f = \sum_{i=1}^{ne} \int_{T_i} f \approx \sum_{i=1}^{ne} \sum_{j=1}^{nq} w_j^{T_i} f(q_j^{T_i}),$$

where nq is the degree of the quadrature rule, $q_j^{T_i}$ are the quadratures points, and $w_j^{T_i}$ are some appropriately chosen weights. Then

$$\left(\langle \phi_j, \phi_i \rangle_{\mathcal{L}}^q\right) c^q = \left(\langle f, \phi_i \rangle^q\right),$$

where $\langle \cdot, \cdot \rangle_{\mathcal{L}}^q$ and $\langle f, \cdot \rangle^q$ denote the quadrature approximation of the bilinear form and linear functional respectively. The solution to this approximated problem is denoted by c^q.

Suppose that the quadrature formula converges to the exact integral as $nq \to \infty$. If $\langle \cdot, \cdot \rangle_{\mathcal{L}}$ is $\mathcal{H}$-elliptic, it follows that $\langle \cdot, \cdot \rangle_{\mathcal{L}}^q$ is V_h-elliptic ($V_h \subset \mathcal{H}$) for nq large enough, which implies that $\left(\langle \phi_j, \phi_i \rangle_{\mathcal{L}}^q\right)$ is invertible. In general, the $\mathcal{H}$-elliptic property of $\langle \cdot, \cdot \rangle_{\mathcal{L}}$ is established using the Sobolev embedding theorems/Poincaré inequalities.

For any polynomial basis and Gaussian quadratures there is nq large enough so that $\langle \phi_j, \phi_i \rangle_{\mathcal{L}}^q = \langle \phi_j, \phi_i \rangle_{\mathcal{L}}$, in which case

$$\|c^q - c\| \leq \left\| \left(\langle f, \phi_i \rangle^q - \langle f, \phi_i \rangle \right) \right\| \left\| \left(\langle \phi_j, \phi_i \rangle_{\mathcal{L}}^q \right)^{-1} \right\|,$$

and approximating $f = p + \epsilon$, with p polynomial, we have

$$\left\| \left(\langle f, \phi_i \rangle^q - \langle f, \phi_i \rangle \right) \right\| \leq 2 \sup(|\epsilon|) \left\| \left(\langle 1, |\phi_i| \rangle \right) \right\|.$$

Bounding the projection error for a polynomial basis of order k requires assumptions about the domain Ω. It follows, for example, by the the Bramble-Hilbert lemma that $\|u - u_h\|_{1,\Omega} = O(h^k)$, where u_h denotes the projection of the solution u to the finite dimensional vector space V_h. Of course, more sophisticated and practical ways of estimating these errors can be found in the literature.

3 Formal power series and the homological equations for parabolic PDEs

We now turn to the main problem of this paper, which is to extend the kinds of calculations illustrated in Section A to the "vector fields" on Sobolev spaces generated by parabolic PDEs. To this end we introduce a fairly simple class of nonlinear heat equations which we find sufficient to highlight the main issues. Nevertheless, the discussion in this section generalizes to parabolic equations involving more general elliptic operators, to problems formulated on spatial domains of three or more dimensions with more general boundary conditions, and even to systems of PDEs. Indeed, our goal in this section is not to describe the most general possible setting but rather to illustrate the application parameterization method, and especially the solution of Eq. (2.5), for an interesting class of PDEs. Some extensions are given in Sect. 4.

Let $\Omega \subset \mathbb{R}^2$ denote bounded, planar, polygonal domain and $f : \mathbb{R} \times \Omega \to \mathbb{R}$ be a smooth function, satisfying mild growth conditions at infinity. Consider the class of scalar parabolic PDEs given by

$$\frac{\partial}{\partial t} u(t, x, y) = \Delta u(t, x, y) + f(u(t, x, y), x, y), \tag{3.1}$$

with the Neumann boundary conditions

$$\frac{\partial}{\partial \mathbf{n}} u(t, x, y) = 0 \quad \text{for } (x, y) \in \partial\Omega.$$

Fix $\mathcal{H} = H^1$. We are interested in the dynamics of the semi-flow generated by the vector field $F : \mathcal{H} \to \mathcal{H}^\vee$ given by

$$F(u) = \Delta u + f(u, x, y).$$

These spaces are appropriate for defining a weak version of $F(u)$.

We now consider an equilibrium solution. That is, suppose that $u_0 : \Omega \to \mathbb{R}$ is in $\mathcal{H}$ and is a solution of the weak form of the elliptic nonlinear boundary value problem

$$\Delta u(x, y) + f(u(x, y), x, y) = 0,$$

subject to the Neumann boundary conditions. More precisely, this means that u_0 satisfies

$$-\int_\Omega \nabla u(x,y)\cdot\nabla\phi(x,y)+\int_\Omega f(u,x,y)\phi(x,y)=0,$$

for all $\phi\in\mathcal{H}$.

Suppose also that u_0 has Morse index M. That is, we assume that $\lambda_1,\dots,\lambda_M\in(0,\infty)$ are the unstable eigenvalues, each with multiplicity one. Let $\xi_1,\dots,\xi_M:\Omega\to\mathbb{R}$ denote associated unstable eigenfunctions, i.e. solutions in $\mathcal{H}$ of the weak form of the eigenvalue problem

$$\Delta\xi(x,y)+\partial_1 f(u_0,x,y)\xi=\lambda\xi(x,y),$$

again subject to the boundary conditions.

We look for $P:[-1,1]^M\to\mathcal{H}$ solving Eq. (2.5), with P given by the formal power series

$$P(\theta_1,\dots,\theta_M,x,y)=\sum_{n_1=0}^{\infty}\dots\sum_{n_M=0}^{\infty}p_{n_1,\dots,n_M}(x,y)\theta_1^{n_1}\dots\theta_M^{n_M}.$$

Here each coefficient $p_{n_1,\dots,n_M}\in\mathcal{H}$ is required to satisfy the boundary conditions. Moreover, imposing the constraints of Eqs. (2.2) and (2.3) gives that the first order coefficients of P are

$$p_{0,\dots,0}(x,y)=u_0(x,y),$$

and

$$p_{1,\dots,0}(x,y)=\xi_1(x,y),\qquad\dots\qquad p_{0,\dots,1}(x,y)=\xi_M(x,y).$$

To work out the higher order coefficients we follow the blueprint of Section A. Begin by letting Λ denote the diagonal matrix of unstable eigenvalues as in Eq. (2.4). Calculating the push forward of Λ by DP on the level of power series gives

$$\begin{aligned}DP(\theta,x,y)\Lambda\theta&=[\partial_1P(\theta,x,y),\dots,\partial_MP(\theta,x,y)]\begin{pmatrix}\lambda_1\theta_1\\ \vdots\\ \lambda_M\theta_M\end{pmatrix}\\&=\lambda_1\theta_1\frac{\partial}{\partial\theta_1}P(\theta,x,y)+\dots+\lambda_M\theta_M\frac{\partial}{\partial\theta_M}P(\theta,x,y)\\&=\sum_{n_1=0}^{\infty}\dots\sum_{n_M=0}^{\infty}(n_1\lambda_1+\dots+n_M\lambda_M)p_{n_1,\dots,n_M}(x,y)\theta_1^{n_1}\dots\theta_M^{n_M}.\end{aligned}$$

Observe that the value of this series at $\theta=0$ is zero.

Next consider

$$F(P(\theta,x,y))=\Delta P(\theta,x,y)+f(P(\theta,x,y),x,y).$$

Proceeding formally, we commute the Laplacian with the infinite sum, and have that

$$\Delta P(\theta,x,y)=\sum_{n_1=0}^{\infty}\dots\sum_{n_M=0}^{\infty}\Delta p_{n_1,\dots,n_M}(x,y)\theta_1^{n_1}\dots\theta_M^{n_M}.$$

If f is analytic then $f(P(\theta, x, y), x, y)$ admits a power series representation. (For f only C^k regularity the argument below is modified accordingly). Let us write

$$f(P(\theta, x, y), x, y) = \sum_{n_1=0}^{\infty} \dots \sum_{n_M=0}^{\infty} q_{n_1,\dots,n_M}(x, y)\theta_1^{n_1} \dots \theta_M^{n_M},$$

where the $q_{n_1,\dots,n_M}$ are the formal Taylor coefficients of the composition, and each depends on the coefficients of P. Efficient computation of the $q_{n_1,\dots,n_M}$ best illustrated through examples in the next section and for the moment we remark that, for any given multi-index $(n_1, \dots, n_M) \in \mathbb{N}^M$, the dependence of $q_{n_1,\dots,n_M}$ on $p_{n_1,\dots,n_M}$ has

$$q_{n_1,\dots,n_M} = D_1 f(u_0, x, y) p_{n_1,\dots,n_M} + S_{n_1,\dots,n_M},$$

where $S_{n_1,\dots,n_M}$ depends only on coefficients of P of lower order. This follows from the Faá di Bruno formula.

Matching like powers in Eq. (2.5) leads to

$$\begin{aligned}
&(n_1\lambda_1 + \dots + n_M\lambda_M) p_{n_1,\dots,n_M} \\
&\quad = \Delta p_{n_1,\dots,n_M} + q_{n_1,\dots,n_M} \\
&\quad = \Delta p_{n_1,\dots,n_M} + D_1 f(u_0, x, y) p_{n_1,\dots,n_M} + S_{n_1,\dots,n_M},
\end{aligned}$$

so that

$$\begin{aligned}
&\Delta p_{n_1,\dots,n_M} + D_1 f(u_0, x, y) p_{n_1,\dots,n_M} - (n_1\lambda_1 + \dots + n_M\lambda_M) p_{n_1,\dots,n_M} \\
&\quad = -S_{n_1,\dots,n_M}.
\end{aligned}$$

That is, $p_{n_1,\dots,n_M}$ solves the linear equation

$$(DF(u_0) - (n_1\lambda_1 + \dots + n_M\lambda_M)\mathrm{Id}_{\mathcal{H}})\, p_{n_1,\dots,n_M} = -S_{n_1,\dots,n_M}, \tag{3.2}$$

where the right hand side depends only on lower order terms.

Equation (3.2) is *the homological equation* for the unstable manifold for F at u_0. Observe that Eq. (3.2) is a linear elliptic PDE with the same boundary conditions as the original reaction/diffusion Eq. (3.1). Indeed, the linear operator on the left hand side is the resolvent of $DF(u_0)$, evaluated at the complex numbers $n_1\lambda_1 + \dots + n_M\lambda_M$. Then each Taylor coefficient of P is the solution of a linear problem no more complicated than the linearized equation at u_0, so that these equations are themselves amiable to finite element analysis under mild assumptions on the domain Ω.

This is a general fact which makes the parameterization method so useful. The homological equations determining the jets of the invariant manifold parameterization are linear equations, as complicated as the linearized problems at the steady state itself. For example when considering a finite dimensional problem in Section A, the steady state equations were systems of n nonlinear algebraic equations in n unknowns, and in this case the homological equations turned out to be systems of n linear equations in n unknowns. Moreover, the homological equations involved the characteristic matrix for the derivative of the vector field at the equilibrium.

In the calculations just discussed, the steady state equation is a nonlinear elliptic BVPs, and the homological equations turn out the be linear elliptic BVPs on the same domain with the same boundary conditions. In fact the linear operator is just the resolvent of the differential, in direct analogy with the finite dimensional case. In the remarks below, we expand on several similarities between the results just derived and the simple example calculation considered in Section A.

Remark 3.1 (Non-resonance conditions and existence of a formal solution) Observe that Eq. (3.2) has a unique solution if and only if the *non-resonance condition*

$$n_1\lambda_1 + \ldots + n_M\lambda_M \notin \text{spec}(DF(u_0)), \tag{3.3}$$

is satisfied whenever $n_1 + \ldots + n_M \geq 2$. Since $\lambda_1, \ldots, \lambda_M$ are the only unstable eigenvalues of $DF(u_0)$, and since $DF(u_0)$ generates a compact semi-group, we have that the countably many remaining eigenvalues are stable. (In practice we check that the remaining eigenvalues of the numerically computed derivative have negative real part).

Since the $n_1, \ldots, n_M$ are all positive, there are only finitely many opportunities for $n_1\lambda_1 + \ldots + n_M\lambda_M$ to be an eigenvalue. If Eq. (3.3) is satisfied for all multi-indices $(n_1, \ldots, n_M) \in \mathbb{N}^M$ with $n_1 + \ldots + n_M \geq 2$ then we say that the unstable eigenvalues are *non-resonant*, and in this case we have that the parameterization P is formally well defined to all orders. That is, Eq. (2.5) has a well defined formal series solution satisfying the first order constraints of Eqs. (2.2) and (2.3).

Remark 3.2 (Uniqueness up to rescaling of the first order data) The unique solvability of the homological equations, assuming non-resonance of the unstable eigenvalues, gives that the solution P at u_0 is unique up to the choice of the scalings of the eigenfunctions. The choice of the scaling of the eigenfunctions directly effects the decay of the coefficients $p_{n_1,\ldots,n_M}$ as discussed in [4, 38]. For this reason we always fix the domain of the parameterization to be $\mathbb{B} = [-1, 1]^M$, and choose the scaling of the eigenvectors so that the coefficients decay rapidly. Of course while choosing smaller scalings for the eigenvectors provides faster coefficient decay, it also means that the image of $\mathbb{B}$ is smaller in $\mathcal{H}$. That is, smaller scalings stabilize the numerics but reveal a smaller portion of the local unstable manifold. In practice we must strike a balance between the polynomial order of the calculation (at what order do we truncate the formal series?) the scaling of the eigenvectors and the size of the local unstable manifold we compute.

3.1 Automatic differentiation of power series

This section deals with the problem of working out the power series coefficients of nonlinear functions of known power series. Classic references for this material (which focus on the one variable case) are [31, 32]. The discussion will focus on the multivariable case.

A critical step in any explicit example application of the parameterization method is to work out the dependence of the coefficients $q_{n_1,\ldots,n_M}$ of the nonlinear composition on the unknown coefficients $p_{n_1,\ldots,n_M}$. This is essential for defining the right hand side $S_{n_1,\ldots,n_M}$ of the Homological equation (3.2). This challenge reduces to repeated application of the Cauchy product formula whenever $f(\cdot, x, y)$ has polynomial nonlinearity.

For example consider the case where f is a quadratic function of the form

$$f(u, x, y) = a(x, y)u^2.$$

Then, the standard Cauchy product formula for two power series gives that

$$\begin{aligned} &f(P(\theta, x, y), x, y) \\ &\quad = a(x, y)\left(\sum_{n_1=0}^{\infty} \cdots \sum_{n_M=0}^{\infty} p_{n_1,\ldots,n_M}(x, y)\theta_1^{n_1} \ldots \theta_M^{n_M}\right) \end{aligned}$$

$$\times \left(\sum_{n_1=0}^{\infty} \cdots \sum_{n_M=0}^{\infty} p_{n_1,\ldots,n_M}(x,y)\theta_1^{n_1}\ldots\theta_M^{n_M} \right)$$
$$= \sum_{k_1=0}^{n_1} \cdots \sum_{k_M=0}^{n_M} q_{n_1,\ldots,n_M}(x,y)\theta_1^{n_1}\ldots\theta_M^{n_M},$$

where

$$\begin{aligned} q_{n_1,\ldots,n_M}(x,y) &= \sum_{k_1=0}^{n_1} \cdots \sum_{k_M=0}^{n_M} a(x,y)p_{n_1-k_1,\ldots,n_M-k_M}(x,y)p_{k_1,\ldots,k_M}(x,y) \\ &= 2a(x,y)p_{0,\ldots,0}(x,y)p_{n_1,\ldots,n_M}(x,y) + \text{“lower order terms”} \\ &= 2\frac{\partial}{\partial u}f(u_0,x,y)p_{n_1,\ldots,n_M}(x,y) + \text{“lower order terms”}, \end{aligned}$$

as promised in the previous section. We see that the “lower order terms” have the explicit form

$$S_{n_1,\ldots,n_M} = \sum_{k_1=0}^{n_1} \cdots \sum_{k_M=0}^{n_M} \hat{\delta}^{k_1,\ldots,k_M}_{n_1,\ldots,n_M} a(x,y)p_{n_1-k_1,\ldots,n_M-k_M}(x,y)p_{k_1,\ldots,k_M}(x,y)$$

where the coefficient

$$\hat{\delta}^{k_1,\ldots,k_M}_{n_1,\ldots,n_M} = \begin{cases} 0 & \text{if } k_1 = \ldots = k_M = 0 \\ 0 & \text{if } k_1 = n_1, \ldots, k_M = n_M \\ 1 & \text{otherwise} \end{cases},$$

appears in the sum to indicate that both of the terms with $p_{n_1,\ldots,n_M}(x,y)$ have been removed.

When f contains non-polynomial terms, calculating the $q_{n_1,\ldots,n_M}$ is more delicate. We employ a semi-numerical technique based on the idea that many typical nonlinearities appearing in applications are themselves solutions of polynomial differential equations. This is exploited in fast recursion schemes.

Consider for example the case of

$$f(u,x,y) = a(x,y)e^{-u}.$$

Let

$$P(\theta,x,y) = \sum_{n_1=0}^{\infty} \cdots \sum_{n_M=0}^{\infty} p_{n_1,\ldots,n_M}(x,y)\theta_1^{n_1}\ldots\theta_M^{n_M},$$

and write

$$Q(\theta,x,y) = \sum_{n_1=0}^{\infty} \cdots \sum_{n_M=0}^{\infty} q_{n_1,\ldots,n_M}(x,y)\theta_1^{n_1}\ldots\theta_M^{n_M} = f(P(\theta,x,y)). \tag{3.4}$$

The following idea is described in detail in Chapter 2 of [24]. We apply the *radial gradient*—the first order partial differential operator given by

$$\nabla_\theta = \theta_1\frac{\partial}{\partial\theta_1} + \ldots + \theta_M\frac{\partial}{\partial\theta_M},$$

to both sides of Eq. (3.4) and obtain

$$\nabla_\theta f(P(\theta,x,y),x,y) = \nabla_\theta Q(\theta,x,y).$$

That is

$$
\begin{aligned}
&\nabla_\theta f(P(\theta,x,y),x,y)\\
&\quad=\theta_1\frac{\partial}{\partial u}f(u,x,y)\,\big|_{u=P(\theta,x,y)}\ \frac{\partial}{\partial\theta_1}P(\theta,x,y)+\ldots\\
&\qquad+\theta_M\frac{\partial}{\partial u}f(u,x,y)\,\big|_{u=P(\theta,x,y)}\ \frac{\partial}{\partial\theta_M}P(\theta,x,y)\\
&\quad=-a(x,y)e^{-P(\theta,x,y)}\left(\theta_1\frac{\partial}{\partial\theta_1}P(\theta,x,y)+\ldots+\theta_M\frac{\partial}{\partial\theta_M}P(\theta,x,y)\right)\\
&\quad=-Q(\theta,x,y)\nabla_\theta P(\theta,x,y)\\
&\quad=-\left(\sum_{n_1=0}^{\infty}\cdots\sum_{n_M=0}^{\infty}q_{n_1,\ldots,n_M}(x,y)\theta_1^{n_1}\ldots\theta_M^{n_M}\right)\\
&\left(\sum_{n_1=0}^{\infty}\cdots\sum_{n_M=0}^{\infty}(n_1+\ldots+n_M)p_{n_1,\ldots,n_M}(x,y)\theta_1^{n_1}\ldots\theta_M^{n_M}\right)\\
&\qquad=-\sum_{n_1=0}^{\infty}\cdots\sum_{n_M=0}^{\infty}\left(\sum_{k_1=0}^{n_1}\cdots\sum_{k_M=0}^{n_M}(k_1+\ldots+k_M)q_{n_1-k_1,\ldots,n_M-k_M}p_{k_1,\ldots,k_M}\right)\theta_1^{n_1}\ldots\theta_M^{n_M},
\end{aligned}
$$

on the left, and

$$\nabla_\theta Q(\theta,x,y)=\sum_{n_1=0}^{\infty}\cdots\sum_{n_M=0}^{\infty}(n_1+\ldots+n_M)q_{n_1,\ldots,n_M}(x,y)\theta_1^{n_1}\ldots\theta_M^{n_M}$$

on the right. Matching like powers and isolating $q_{n_1,\ldots,n_M}$ leads to

$$q_{n_1,\ldots,n_M}=\frac{-1}{n_1+\ldots+n_M}\sum_{k_1=0}^{n_1}\cdots\sum_{k_M=0}^{n_M}(k_1+\ldots+k_M)q_{n_1-k_1,\ldots,n_M-k_M}p_{k_1,\ldots,k_M}.$$

Then the complexity of computing the power series coefficients of $a(x,y)e^{-P(\theta,x,y)}$ is the complexity of a single Cauchy product. The additional cost is that the coefficients of Q have to be stored in addition to those of P.

Such methods for formal series manipulations are referred to by many authors as *automatic differentiation for power series*, and they facilitate rapid computation of the formal series coefficients of compositions with all the elementary functions. A classic reference, which includes an in depth historical discussion, is found in Chapter 4, Section 6 of [32]. See also the discussion of software implementations found in [31].

4 Applications

4.1 A first worked example: Fisher's Equation

Consider the parabolic PDE

$$\frac{\partial}{\partial t}u=\Delta u+\alpha u(1-u),$$

on the $\mathbb{L}$ domain Ω illustrated in the left-most frame of Fig. 3, subject to the Neumann boundary conditions

$$\nabla u \cdot \mathbf{n}|_{\partial\Omega} = 0.$$

Here $\mathbf{n}$ is a unit vector normal to $\partial\Omega$. This reaction-diffusion equation was introduced by Ronald Fisher in the context of population dynamics, as a toy model for the propagation of advantageous genes. It is essentially a nonlinear heat equation with logistic nonlinearity. Letting

$$F(u) = \Delta u + \alpha u(1-u),$$

we see that the problem describes an evolution equation as in Eq. (2.1). For this example we let $\mathcal{H} = H^1(\Omega)$.

The example provides an interesting first study both because it has the simplest possible nonlinearity, and also because the well understood bifurcation structure of the problem gives us easy access to non-trivial equilibrium solutions with any desired Morse index as we now discuss.

Recall that an equilibrium solution has $F(u) = 0$, so that the constant function 0 is always an equilibrium solution of Fisher's Equation. This is referred to as the homogeneous background solution. Note that when $\alpha = 0$, the homogeneous background solution is stable, as the problem reduces to the heat equation. For $\alpha \neq 0$ the problem has two constant equilibrium solutions, $u \equiv 0$ and $u \equiv 1$.

Increasing α causes an eigenvalue to crosses the imaginary axis (in fact it pass through zero as all eigenvalues are real) so that the homogeneous background solution looses stability. This is a symmetry breaking, or pitch-fork bifurcation and it gives rise to a pair of non-constant equilibrium solutions. The new branches of equilibrium solutions carry the pre-bifurcation Morse index of background state, so that after the first bifurcation they are stable. The eigenvalue-eigenvector problem is specified below.

As α increases more and more eigenvalues pass through zero, increasing the morse index of the homogeneous solution. Each of these bifurcations gives rise to a new branch of equilibrium solutions, and we can follow any of these branches using numerical continuation methods. The first pair of non-trivial equilibria to appear are initially stable, however they also undergo symmetry breaking bifurcations of their own, and loose stability as α is increased further. For example, at $\alpha = 2.7$ the first non-trivial branch of equilibrium solutions have Morse index 1, and Morse index 2 when $\alpha = 9$. These equilibrium solutions then have one and two dimensional attached unstable manifolds respectively. In the remainder of this section we discuss in detail the parameterization of the two dimensional unstable manifold for this otherwise simple example.

To find equilibria, we study the nonlinear elliptic BVP

$$F(u) = \Delta u + \alpha u(1-u) = 0,$$

subject to the same natural boundary conditions on Ω. The weak formulation is

$$\mathcal{F}(u)\phi = -\int_\Omega \nabla u \cdot \nabla\phi + \int_\Omega \alpha u(1-u)\phi = 0,$$

and, using the notation of Sect. 2.2, triangulate Ω and solve for the coefficients of the finite element representation $u_h = \sum_{j=1}^{nb} c_j\phi_j$ of u. In order to construct this projection, define

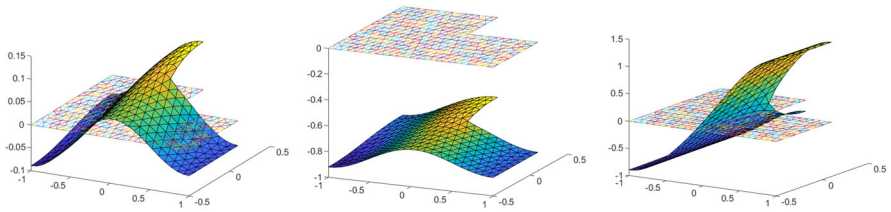

Fig. 4 Fisher's equation with $\alpha = 9$, $ne = 515$. Left: Equilibrium solution, with Morse index 2. Center: Eigenfunction for $\lambda_1 = 9.04$. Right: Eigenfunction for $\lambda_2 = 7.16$

the linear basis functions ϕ_j as

$$\phi_j(n_i) = \begin{cases} 1 & j = i \\ 0 & j \neq i \end{cases},$$

where n_i denotes the $i-th$ vertex in the triangulation. Note that in this case, $nb = nn$. Letting $\phi = \phi_i$ for $1 \leq i \leq nb$ leads to the nonlinear system of nb equations in nb unknowns, given by

$$\mathcal{F}_i^h(c) = -\int_\Omega \left(\sum_{j=1}^{nb} c_j \nabla\phi_j\right) \cdot \nabla\phi_i + \int_\Omega \alpha \left(\sum_{j=1}^{nb} c_j\phi_j\right)\left(1 - \sum_{j=1}^{nb} c_j\phi_j\right)\phi_i = 0,$$

which we solve using the Newton's Method (for $c = (c_1, c_2, ..., c_{nb})$). More precisely, let $\mathcal{F}^h(c) = (\mathcal{F}_1^h(c), ..., \mathcal{F}_{nn}^h(c)) = (\mathcal{F}(u_h)\phi_1, ..., \mathcal{F}(u_h)\phi_{nn})$. The k'th Newton's step is given by

$$c^{(k)} = c^{(k-1)} - D\mathcal{F}^h\left(c^{(k-1)}\right)^{-1} \mathcal{F}^h\left(c^{(k-1)}\right),$$

where $u_h^{(k)} = \sum_{j=1}^{nb} c_j^{(k)}\phi_j$ and $D\mathcal{F}^h(c) = -\left(\int_\Omega \nabla\phi_j \cdot \nabla\phi_i\right) + \left(\int_\Omega \frac{\partial N(c)}{\partial c_j}\phi_i\right)$.

Once the approximate solution u_0 is computed we proceed to solve the eigenvalue-eigenvector problem

$$\Delta\xi + \alpha(1 - 2u_0)\xi - \lambda\xi = 0, \qquad \nabla\xi \cdot \mathbf{n}|_{\partial\Omega} = 0.$$

That is, we compute the projection $\xi_h = \sum_{j=1}^{nb} c_j\phi_j$ in the weak formulation, which leads to

$$-\int_\Omega \left(\sum_{j=1}^{nb} c_j \nabla\phi_j\right) \cdot \nabla\phi_i + \int_\Omega \alpha(1 - 2u_0)\left(\sum_{j=1}^{nb} c_j\phi_j\right)\phi_i = \int_\Omega \lambda \left(\sum_{j=1}^{nb} c_j\phi_j\right)\phi_i$$

or

$$\left(-\int_\Omega \nabla\phi_j \cdot \nabla\phi_i + \alpha(1 - 2u_0)\phi_j\phi_i\right)c = \lambda\left(\int_\Omega \phi_j\phi_i\right)c.$$

After computing the unstable eigenvalues λ_1 and λ_2 and the associated eigenfunctions ξ_1 and ξ_2, we proceed to solve the invariance Eq. (2.5) specialized to the present situation. That is, we consider the weak form of the equation

$$F(P(\theta)) = \lambda_1\theta_1 \frac{\partial}{\partial\theta_1} P(\theta) + \lambda_2\theta_2 \frac{\partial}{\partial\theta_2} P(\theta),$$

where

$$P(\theta) = \sum_{m=0}^{\infty} \sum_{n=0}^{\infty} p_{m,n}(x, y)\theta_1^m \theta_2^n,$$

with $p_{0,0} = u_0$, $p_{1,0} = \xi_1$ and $p_{0,1} = \xi_2$. Taking the projection $p_{m,n} = \sum_{j=1}^{nb} c_j^{(m,n)} \phi_j$, leads to

$$\Big(- \int_\Omega \nabla \phi_j \cdot \nabla \phi_i + \alpha(1 - 2u_0 - m\lambda_1 - n\lambda_2)\phi_j \phi_i \Big) \Big(c_i^{(m,n)} \Big) = \Big(\int_\Omega s_{(m,n)} \phi_i \Big),$$

for $m + n \geq 2$, which is

$$\Big(D\mathcal{F}^h(c^{(0)}) - (\lambda_1 m + \lambda_2 n) \int_\Omega \phi_j \phi_i \Big) c^{(m,n)} = \Big(\int_\Omega s_{(m,n)} \phi_i \Big),$$

with

$$s_{(m,n)} = \alpha \sum_{i=0}^{m} \sum_{j=0}^{n} \delta(i, j) p_{i,j} p_{m-i,n-j},$$

and

$$\delta(i, j) = \begin{cases} 0 & (i, j) = (0, 0) \text{ or } (i, j) = (m, n) \\ 1 & \text{otherwise} \end{cases}.$$

As anticipated in Sect. 3.1, the homological equations are linear elliptic PDEs, and we solve them recursively to any desired order using the Finite Element Method. Figure 6 shows a few functions in the *fast manifold* (1d manifold associated to the largest positive eigenvalue) and *slow manifold* (1d manifold associated to the smallest positive eigenfunction) approximated up to order $N = 30$.

The effect of the scaling of the eigenvectors on the decay of the coefficients is illustrated in Fig. 5 .

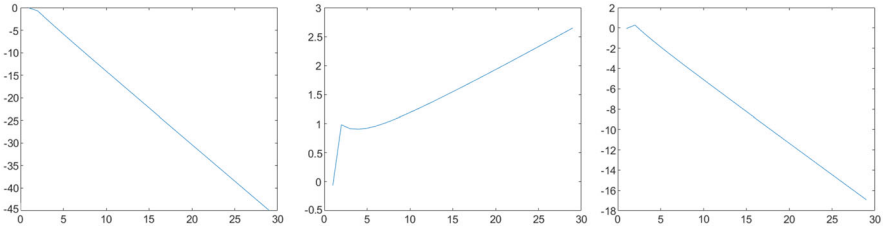

Fig. 5 Coefficient growth: three plots of the magnitude of the parameterization coefficients as a function of the order of the coefficients. (Horizontal axis is the order of the coefficient and vertical axis is the base ten logarithm L^2 norm of the coefficient function). Left: The scaling of the eigenvector is too small, and the coefficients decay too fast. Coefficients after order then are below machine precision in L^2 norm (smaller than 10^{-16}) and hence do not contribute significantly to the accuracy of the polynomial approximation. Center: The eigenvector scaling is choosen too large, and now the $p_{m,n}$'s grow exponentially fast. This introduces numerical instabilities into the approximation. Right: The scaling is chosen just right: they decay exponentially fast at a rate chosen so that the N-th order coefficients reach machine precision

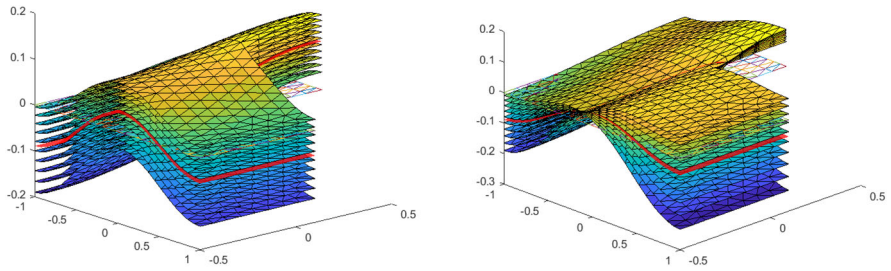

Fig. 6 Left: 10 functions on the fast manifold approximated to order $N = 30$ with Invariance equation error of 1.34e−8 with respect to the L^2 norm, and 5.98*e−8 with respect to the H^1 norm. Right: 10 functions on the slow manifold approximated to order $N = 30$ with Invariance equation error of 4.56e−07 with respect to the L^2 norm, and 2.19e−06 with respect to the H^1 norm

4.2 A reaction diffusion equation with non-polynomial nonlinearity: one unstable eigenvalues

In this section we derive the homological equations for a non-polynomial problem. We consider the reaction diffusion equation with Ricker type exponential nonlinearity given by

$$u_t = \Delta u + \alpha u \left(0.5 - e^{-u}\right), \tag{4.1}$$

over the $\mathbb{L}$ domain with Neumann boundary conditions and $\mathcal{H} = H^1(\Omega)$.

We refer to this problem as the Fisher-Ricker (FR) equation, and take parameter $\alpha = -4.7$. Letting

$$F(u) = \Delta u + \alpha u \left(0.5 - e^{-u}\right),$$

we obtain an evolution equation of the kind given in Eq. (2.1).

To find the equilibrium solution consider the weak form of the equation $F(u) = 0$, project into a finite element space of piecewise linear functions, and solve

$$\mathcal{F}_i^h(c) = -\int_\Omega \left(\sum_{j=1}^{nb} c_j \nabla\phi_j\right)\cdot\nabla\phi_i + \int_\Omega \alpha\left(\sum_{j=1}^{nb}\phi_j\right)\left(0.5 - \exp\{-\sum_{j=1}^{nb} c_j\phi_j\}\right)\phi_i = 0.$$

The corresponding eigenvalue-eigenfunction problem is

$$D\mathcal{F}^h(c^{(0)})c = \lambda\Big(\int_\Omega \phi_j\phi_i\Big)c.$$

Suppose now that u_0 is an equilibrium solution with Morse index 1, let λ denote the unstable eigenvalue, and ξ be a corresponding eigenfunction. We seek a parameterization of the form $P(\theta) = \sum_{n=0}^{\infty} p_n\theta^n$ solving the 1D Invariance Equation

$$F(P(\theta)) = \theta\lambda\frac{d}{d\theta}P(\theta),$$

which, after expanding $P(\theta)$ as a power series becomes

$$\sum_{n=0}^{\infty}\Delta p_n\theta^n + \alpha\left(\sum_{n=0}^{\infty}p_n\theta^n\right)\left(0.5 - \exp\left(-\sum_{n=0}^{\infty}p_n\theta^n\right)\right) = \lambda\sum_{n=0}^{\infty}np_n\theta^n.$$

Here, the $p_n = p_n(x, y)$ are functions defined on Ω satisfying the boundary conditions.

We compute the power series coefficients of the exponential nonlinearity as in Sect. 3.1. That is, we introduce the new variable

$$Q(\theta) := e^{-P(\theta)} = \sum_{n=0}^{\infty} q_n \theta^n,$$

and note that $Q' = -QP'$. Then

$$q_n = -p_n q_0 - \frac{1}{n} \sum_{j=0}^{n-2} (j+1) p_{j+1} q_{n-1-j}. \tag{4.2}$$

Note that Eq. (4.2) involves only sums and products of the functions $p_i(x, y), q_j(x, y)$, for $0 \le i, j \le n$, and that these operations are well defined for p_n, q_n in any finite element space. Equation (4.2) then allows us to compute q_n to any desired order, assuming that $p_n, \ldots, p_0$, and $q_{n-1}, \ldots, q_0$ are known.

Returning to the Invariance Equation and using the recursive formula for q_n we obtain that for $n \ge 2$, the p_n solve

$$\Delta p_n + \alpha(0.5 - q_0 - \lambda n) p_n - \alpha p_0 q_n = \alpha \sum_{j=1}^{n-1} p_j q_{n-j},$$

or

$$\Delta p_n + \alpha(0.5 - q_0 + p_0 q_0 - \lambda n) p_n = s_n,$$

where

$$s_n = \alpha \sum_{j=1}^{n-1} p_j q_{n-j} - \frac{\alpha p_0}{n} \sum_{j=0}^{n-2} (j+1) p_{j+1} q_{n-1-j}.$$

Passing to the weak form, we find that the coefficients $p_n = \sum_{j=1}^{nb} c_j^{(n)} \phi_j$ solve the homological equations

$$\left(D\mathcal{F}^h(c^{(0)}) - \lambda n \int_\Omega \phi_j \phi_i \right) c^{(n)} = \left(\int_\Omega s_n \phi_i \right), \tag{4.3}$$

for $n \ge 2$. Notice that s_n only depends on p_k's and q_k's with $0 < k < n$. Then if $p_0, \ldots, p_{n-1}$ and $q_0, \ldots, q_{n-1}$ are known, p_n is computed by solving Eq. (4.3). Once p_n is known, we update Eq. (4.2) to obtain q_n.

4.3 A reaction diffusion equation with non-polynomial nonlinearity:two unstable eigenvalues

A modification of the method just discussed allows us to compute higher dimensional manifolds in problems with non-polynomial nonlinearities. Consider again Eq. (4.1),

this time with $\alpha = -4.41$. At this parameter value there is a non-trivial equilibrium u_0 with Morse index 2. Let λ_1 and λ_2 denote the unstable eigenvalues and ξ_1, ξ_2 denote an associated pair of unstable eigenfunctions.

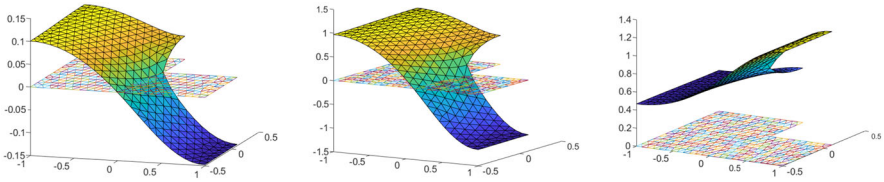

Fig. 7 Fisher-Ricker equation with $\alpha = -4.7$, $ne = 515$. Left: Equilibrium solution. Center: Eigenfunction ξ_1 with $\lambda_1 = 2.41$. Right: Eigenfunction ξ_2 with $\lambda_2 = 0.05$

Recall that for an equilibrium with Morse index 2, the invariance equation becomes

$$F(P(\theta)) = \lambda_1\theta_1\frac{\partial}{\partial\theta_1}P(\theta) + \lambda_2\theta_2\frac{\partial}{\partial\theta_2}P(\theta),$$

and we seek a power series solution of the form

$$P(\theta) = \sum_{m=0}^{\infty}\sum_{n=0}^{\infty} p_{m,n}(x, y)\theta_1^m\theta_2^n,$$

with

$$p_{00} = u_0, \qquad p_{10} = \xi_1, \quad \text{and} \quad p_{01} = \xi_2,$$

and where $p_{m,n}$ for $m + n \geq 2$ are to be determined.

Once again, we exploit the technique developed in Sect. 3.1 to work out the exponential nonlinearity, and define the auxiliary equation

$$Q := \exp(-P(\theta)) = \sum_{m=0}^{\infty}\sum_{n=0}^{\infty} q_{m,n}(x, y)\theta_1^m\theta_2^n,$$

and take the radial gradient to obtain that

$$q_{m,n} = -\frac{1}{(m+n)}\sum_{i=1}^{m}\sum_{j=1}^{n}(i + j)p_{i,j}q_{m-i,n-j}.$$

Note that this requires only additions and multiplications, all well defined operations for finite element basis functions.

Returning to the Invariance Equation and using the recursive formula for $q_{m,n}$ we have

$$\Delta p_{m,n} + \alpha(0.5 - q_{0,0} - \lambda_1 m - \lambda_2 n)p_{m,n} - \alpha p_{0,0}q_{m,n} = \alpha\sum_{i=0}^{m}\sum_{j=0}^{n} q_{i,j}p_{m-i,n-j}\delta(i, j),$$

so that the strong form of the homological equation is

$$\Delta p_{m,n} + \alpha(0.5 - q_{0,0} + p_{0,0}q_{0,0} - \lambda_1 m - \lambda_2 n)p_{m,n} = s_{m,n},$$

with

$$s_{m,n} = \alpha\sum_{i=0}^{m}\sum_{j=0}^{n} q_{i,j}p_{m-i,n-j}\delta(i, j) - \frac{\alpha p_{0,0}}{(m+n)}\sum_{i=1}^{m-1}\sum_{j=1}^{n-1}(i + j)p_{i,j}q_{m-i,n-j},$$

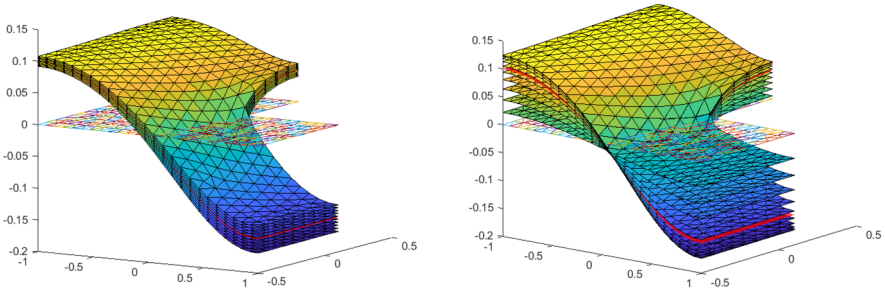

Fig. 8 Left: 10 functions on the fast manifold approximated to order $N = 30$ with Invariance equation error of 9.21e−8 with respect to the L^2 norm, 3.69e−07 with respect to the H^1 norm. Right: 10 functions on the slow manifold approximated to order $N = 30$ with Invariance equation error of 6.12e−06 with respect to the L^2 norm, 2.50e−05 with respect to the H^1 norm

a linear, elliptic BVP for each $m + n \geq 2$ as desired. Passing to the weak form leads to

$$\Big(D\mathcal{F}^h(c^{(0)}) - (\lambda_1 m + \lambda_2 n)\int_\Omega \phi_j\phi_i\Big)c^{(m,n)} = \Big(\int_\Omega s_n\phi_i\Big),$$

which we solve recursively via the finite element method, obtaining the parameterization coefficients to any desired order (updating the equation for q_{mn} as we go). Results are illustrated in Fig. 8.

4.4 Higher order PDEs: a Kuramoto-Sivashinsky small term

We now consider a higher order problem, with leading diffusion term given by the biharmonic Laplacian. The biharmonic operator often appears in models of thin structures that react elastically to external forces. The Kuramoto-Sivashinsky equation (or KS equation) is given by

$$\begin{aligned} F(u) &= -\Delta^2 u - \Delta u - 0.5|\nabla u|^2, \\ u|_{\partial\Omega} &= 0 \qquad \nabla u \cdot \mathbf{n}|_{\partial\Omega} = 0. \end{aligned}$$

for $u \in H_0^2(\Omega)$. It models flame front propogation, and is known to exhibit chaotic dynamics. We refer to [30, 34, 35, 47, 60] for more complete discussion of the physics and dynamics of the KS equation.

Since the differential operator is fourth order, higher regularity Finite Elements are required. The purpose of this section is to illustrate the use of the parameterization method in a higher order problem. To simplify the discussion, we start with a known solution of Fisher, and introduce the biharmonic term and nonlinearity as a perturbation with Neumann boundary conditions.

Specifically, we consider $u \in H^2(\Omega)$ and take

$$F_0(u) = \Delta u + \alpha u(1-u) \qquad \nabla u \cdot \mathbf{n}|_{\partial\Omega} = 0,$$

with weak formulation

$$\mathcal{F}_0(u)\phi = -\int_\Omega \nabla u \cdot \nabla\phi + \int_\Omega \alpha u(1-u)\phi = 0,$$

and let $\mathcal{F}_\epsilon(u) \in H^2(\Omega)^\vee$ for the perturbation problem given by

$$\mathcal{F}_\epsilon(u)\phi = \mathcal{F}_0(u)\phi + \int_\Omega \epsilon_1 \Delta u \Delta\phi + \int_\Omega \epsilon_2 N(u)\phi = 0.$$

Notice that regular enough solutions of the weak equation above correspond to strong solutions (with $\beta = 1$) of the problem

$$F_\epsilon(u) = \epsilon_1 \Delta^2 u + \beta \Delta u + \alpha u(1-u) + \epsilon_2 N(u) = 0,$$

with Neumann boundary conditions.

Indeed, starting with

$$\int_\Omega \epsilon_1 \left(\Delta^2 u\right)\phi + \int_\Omega \beta(\Delta u)\phi + \int_\Omega (\alpha u(1-u) + \epsilon_2 N(u))\phi = 0,$$

and applying Green's formula we have:

$$\begin{aligned}\int_\Omega -\epsilon_1 \nabla(\Delta u)\cdot\nabla\phi + \oint_{\partial\Omega} \epsilon_1(\nabla(\Delta u)\cdot n)\phi \\ - \int_\Omega \beta\nabla u\cdot\nabla\phi + \oint_{\partial\Omega} \beta(\nabla u\cdot n)\phi + \int_\Omega (\alpha u(1-u) + \epsilon_2 N(u))\phi = 0.\end{aligned}$$

Assuming that the boundary integrals vanish, we apply Green's formula once more and now have:

$$\int_\Omega \epsilon_1 \Delta u\Delta\phi - \oint_{\partial\Omega} \epsilon_1(\nabla\phi\cdot n)\Delta u - \int_\Omega \beta\nabla u\cdot\nabla\phi + \int_\Omega (\alpha u(1-u) + \epsilon_2 N(u))\phi = 0.$$

Noting that the boundary integral vanish , we obtain the weak equations

$$\int_\Omega \epsilon_1 \Delta u\Delta\phi - \int_\Omega \beta\nabla u\cdot\nabla\phi + \int_\Omega (\alpha u(1-u) + \epsilon_2 N(u))\phi = 0,$$

i.e

$$\int_\Omega \epsilon_1 \Delta u\Delta\phi - \int_\Omega \beta\nabla u\cdot\nabla\phi + \int_\Omega \alpha u\phi = \int_\Omega (\alpha u^2 - \epsilon_2 N(u))\phi.$$

In this last form, one easily identify the perturbation problem from Fisher's equation, $u_t = F_\epsilon(u)$, where

$$F_\epsilon(u) = \epsilon_1 \Delta^2 u + \beta\Delta u + \alpha u(1-u) + \epsilon_2 N(u) = F_0(u) + \epsilon_1 \Delta^2 u + \epsilon_2 N(u).$$

We will choose $N(u) = -0.5|\nabla u|^2$ for our computations (and $\beta = 1$), and ϵ_1 will be a small negative parameter. In this way, for $\beta = 0$ and $\alpha = 0$ (and with Dirichlet boundary conditions instead) we recover the Kuramoto-Sivashinsky model. On the other hand, with $\epsilon_1 = 0$ and $\epsilon_2 = 0$ we obtain again Fisher's equation.

Remark 4.1 The computations in the Matlab scripts are formulated as $u_t = -\alpha\Delta^2 u - \beta\Delta u + \mu u(1-u) - \delta 0.5|\nabla u|^2$, with α small and positive, β negative of absolute value close to 1, μ close to the parameters used for Fisher's equation, and δ small and positive.

Because the weak form of the equation contains the Laplacian (instead of just the gradient) we use C^1 Argyris elements which offer high convergence rate. We refer to [16] for the mathematical theory of the Argyris elements and to [18] for a useful discussion of numerical the implementation.

We recall that the Argyris elements are fifth order polynomials in two space variable constructed as follows. Define the operators $L_1 = id$, $L_2 = \partial_{10}$, $L_3 = \partial_{01}$, $L_4 = \partial_{20}$, $L_5 = \partial_{11}$ and $L_6 = \partial_{02}$. For an element $[n_1, n_2, n_3, m_1, m_2, m_3]$ with nodes n_1, n_2 and n_3 and midpoints of the edges m_1, m_2 and m_3, the nodal basis $\phi_k^{n_i}$ are defined by

$$L_\ell(\phi_k^{n_i}(n_j)) = \delta_{ij}\delta_{\ell k},$$
$$\frac{\partial}{\partial n}\phi_k^{n_i}(m_j) = 0,$$

and the basis associated to the edge midpoints by

$$\frac{\partial}{\partial n}\phi^{m_i}(m_j) = \delta_{ij},$$
$$L_\ell\phi^{m_i}(n_j) = 0,$$

where $1 \le i, j \le 3$ and $1 \le k, \ell \le 6$.

These are 21 constraints for each ϕ which uniquely defines a fifth order polynomials of the form

$$\phi(x, y) = \sum_{0 \le i+j \le 5} c_{ij} x^i y^j.$$

We solve a 21×21 linear system $Ac = b$ for the coefficients c_{ij} for each of the 21 basis associated with an element. In practice, we only do this for a reference triangle and transfer these basis to an arbitrary element using the method of Dominguez and Sayas [18].

In the notation presented earlier, $S_i = \{L_k : 1 \le k \le 6\}$ for $i = 1, 2, 3$ and $S_i = \{\frac{\partial}{\partial n}\}$ for $i = 4, 5, 6$. After some indexing and renaming we let $S = \bigcup_i S_i = \{L_k\}$ and

$$\phi_i = \frac{det(A_i)}{det(A)}$$

for $1 \le i \le 21$. Recall that the coordinates of A, $A_{ij} = \left(L_i(x^m y^n)(z_{n(i)})\right)$, and the coordinates of $A_k, (A_k(x, y))_{ij} = (1-\delta_{ki})A_{ij} + \delta_{ki}x^m y^n$, where $j = \frac{(m+n)(m+n+1)}{2} + (n+1)$.

The global representation of u becomes:

$$u = \sum_{k=1}^{6} \sum_{\text{all } n_i} c_k^{n_i}\phi_k^{n_i} + \sum_{\text{all } m_i} c^{m_i}\phi^{m_i}.$$

This interpolation is indexed in some convenient way: $u = \sum_{j=1}^{nb} c_j\phi_j$ with $nb = 6nv + ned$ where nv is the number of vertices and ned is the number of edges in the triangulation.

After computing an equilibrium solution and eigendata λ and ξ as in the previous examples, we proceed to solve Eq. (2.5) in the case of Morse index one, interpreted in $H^2(\Omega)^\vee$ as

$$F(P(\theta)) = \lambda\theta\frac{\partial P}{\partial\theta}.$$

First comparing powers and then solving for

$$p_n = \sum_{j=1}^{nb} c_j^{(n)}\phi_j,$$

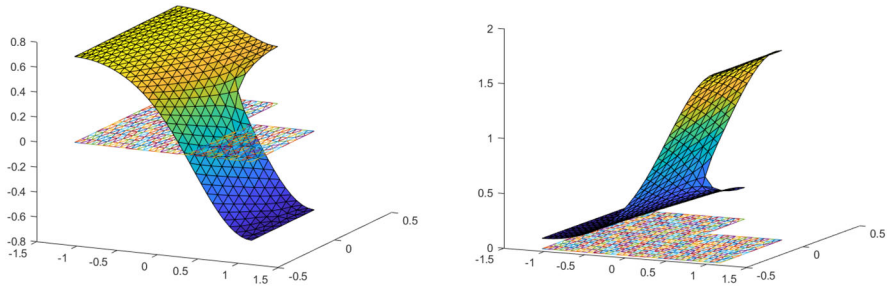

Fig. 9 FKS equation with $\epsilon_1 = -10^{-2}, \beta = 1, \alpha = 2.61$, and $\epsilon_2 = 10^{-3}$ Left: Equilibrium solution, ne=705. Right: Eigenfunction ξ with $\lambda = 3.48$

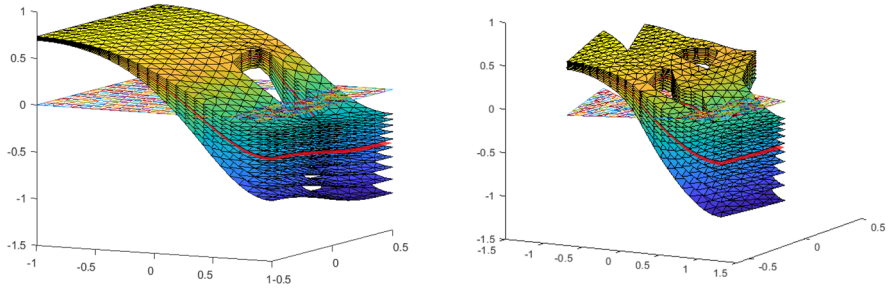

Fig. 10 Unstable manifolds for the FKS equation posed on non-convex domains with holes. Left: $ne = 522$, $\epsilon_1 = -10^{-3}, \beta = 1, \alpha = 3$, and $\epsilon_2 = 10^{-4}$, 10 points on the 1d manifold, $N = 30$. L^2 error on the invariance equation 1.48e−07, H^1 error on the invariance equation 1.17e−06. Right: $ne = 391$, $\epsilon_1 = -10^{-2}, \beta = 1$, $\alpha = 3$, and $\epsilon_2 = 10^{-3}$, 10 points on the 1d manifold, $N = 30$. L^2 error on the invariance equation 1.13e−06, H^1 error on the invariance equation 1.57e−05

leads to

$$\langle \epsilon_1 \Delta^2 p_n + \beta \Delta p_n + \alpha(1 - 2p_0)p_n - \epsilon_2 \left(\frac{\partial p_0}{\partial x} \frac{\partial p_n}{\partial x} + \frac{\partial p_0}{\partial y} \frac{\partial p_n}{\partial y} \right) - \lambda p_n, \phi \rangle = \langle s_n, \phi \rangle$$

where

$$s_n = \frac{\epsilon_2}{2} \left(\sum_{k=1}^{n-1} \frac{\partial p_k}{\partial x} \frac{\partial p_{n-k}}{\partial x} + \frac{\partial p_k}{\partial y} \frac{\partial p_{n-k}}{\partial y} \right) - \alpha \sum_{k=1}^{n-1} p_k p_{n-k},$$

and so the projected weak formulation of the homological equation is of the form

$$\left(D\mathcal{F}^h(c^{(0)}) - \lambda n \int_\Omega \phi_j \phi_i \right) c^{(n)} = \left(\int_\Omega s_n \phi_i \right).$$

In the Fig. 10, we show the manifolds computed over two additional irregular domains. In Fig. 11 the manifold is approximated to order 10 and 120, using the same scaling of the eigenvector. The error improves significantly by increasing the order of the approximation. Equivalently, if we set a tolerance level for the error in our computations, the local manifold obtained for order 10 is significantly smaller.

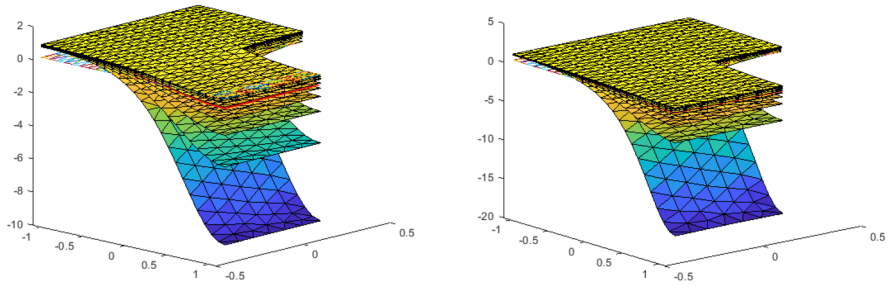

Fig. 11 Unstable manifold for the FKS equation on the $\mathbb{L}$ domain with eigenvector scaled by 0.8 and parameters $\epsilon_1 = -10^{-2}$, $\beta = 1$, $\alpha = 2.61$, and $\epsilon_2 = 10^{-3}$ Left: 10 points on the 1d manifold, $N = 10$, Invariance equation error L^2 norm 0.012, H^1 norm 0.075. Right: 10 points on the 1d manifold, $N = 120$, Invariance equation error L^2 norm 1.55e−05, H^1 norm 1.49e−04

4.5 A-posteriori error estimation

In this section we define a-posteriori error indicators for the parameterization method and illustrate their use in the examples from above. For the first indicator, consider the L^2 norm of the defect associated with the invariance equation. That is, for the N-th order parameterization

$$P^N(\theta, x, y) = \sum_{n=0}^{N} p_n(x, y)\theta^n,$$

of a 1D unstable manifold, define the defect function

$$E_{1,N}(\theta, x, y) := F(P_N(\theta, x, y)) - \lambda\theta \frac{\partial}{\partial\theta} P_N(\theta, x, y),$$

for $\theta \in (-1, 1)$ and $(x, y) \in \Omega$, and the L^2 indicator

$$\epsilon_{N,1} = \int_{|\theta|\leq 1} \left\| E_{1,N}(\theta) \right\|_{L^2(\Omega)}.$$

Note that $\epsilon_{N,1} = 0$ for an exact solution.

Similarly we define, for the parameterization

$$P^N(\theta_1, \theta_2, x, y) = \sum_{m+n=0}^{N} p_{mn}(x, y)\theta_1^m\theta_2^n,$$

of a two dimensional unstable manifold, the defect function

$$E_{N,2}(\theta_1, \theta_2, x, y) = F(P_N(\theta_1, \theta_2, x, y)) - \lambda_1\theta_1 \frac{\partial}{\partial\theta_1} P_N(\theta_1, \theta_2, x, y)$$
$$-\lambda_2\theta_2 \frac{\partial}{\partial\theta_2} P_N(\theta_1, \theta_2, x, y),$$

and the indicator

$$\epsilon_{N,2} = \int_{|\theta_1|,|\theta_2|\leq 1} \left\| E_{2,N}(\theta_1, \theta_2) \right\|_{\mathcal{H}}.$$

In practice these indicators are approximated by computing the $L^2(\Omega)$ norms and average for a finite number of parameter points.

Table 1 L^2, H^1 norms of the error in the Invariance Equation for 1d and 2d unstable manifolds in the Fisher model over the $\mathbb{L}$ domain: $\alpha = 2.7$, $\alpha = 9$ respectively

ne	Fisher 1d manifold $\mathbb{L}$	Fisher 2d manifold $\mathbb{L}$
515	4.922499e−07, 2.550765e−06	5.960955e−07, 2.8448771e−06
984	1.448931e−07, 7.490640e−07	1.560992e−07, 7.498196e−07
1963	3.294838e−08, 2.066328e−07	4.020046e−08, 2.373396e−07

Another class of indicators is obtained by considering the dynamical conjugacy error discussed in Equation (2.6). That is, with fixed $T > 0$ define the dynamical defect

$$\text{conjError}(T)_{N,1}(\theta, x, y) = P^N(e^{\lambda T}\theta, x, y) - \Phi(P^N(\theta, x, y), T),$$

$\theta \in (-1, 1)$ and $(x, y) \in \Omega$, for the 1D manifold and

$$\text{conjError}(T)_{N,2}(\theta_1, \theta_2, x, y) = P^N(e^{\lambda_1 T}\theta_1, e^{\lambda_2 T}\theta_2, x, y) - \Phi(P^N(\theta_1, \theta_2, x, y), T),$$

$\theta_1, \theta_2 \in [-1, 1] \times [-1, 1]$ and $(x, y) \in \Omega$ for the 2D manifold. Then we have the indicators

$$\varepsilon_{N,1} = \sup_{|\theta| \in [-1,1]} \left\| \text{conjError}(T)_{N,1}(\theta) \right\|_{\mathcal{H}},$$

and

$$\varepsilon_{N,2} = \sup_{|\theta_1|, |\theta_2| \leq 1} \left\| \text{conjError}(T)_{N,2}(\theta_1, \theta_2) \right\|_{\mathcal{H}}$$

Note that the calculation of these indicators depends on the (fairly arbitrary) choice of T, and more over requires numerical approximation of the flow map $\Phi(P(\theta, x, y), t)$, which in turn requires implementation of a numerical integration scheme for the parabolic PDE. Then the computation of the ϵ-indicators is in general much simpler than the ε-indicators. For this reason, we much prefer the former in the present work. Nevertheless, the latter can be very valuable for debugging purposes, and we always check the conjugacy errors before claiming with confidence that we have working codes.

Tables 1 - 6 below report the results of a number of defect calculations for the manifold computations of the previous section. We observe that in general the defect decreases as the number of elements increases (and hence the mesh size decreases) and tends to improve as the order N of the approximation increases. It should also be stressed that using finite elements of higher order in a given problem seems to have a dramatic effect on the error. This is illustrated in Table 6, which compares the defect for the 1D manifold in the Fisher equation using piecewise linear versus Argyris elements. While the piecewise linear elements proved approximately 6 figures of accuracy on the L-shaped domain, using the higher order elements

Table 2 L^2, H^1 norms of the error in the Invariance Equation for 1d and 2d manifolds in the Fisher model with exponential nonlinearity over the $\mathbb{L}$ domain: $\alpha = -4.7$, $\alpha = -4.41$ respectively

ne	FR 1d manifold $\mathbb{L}$	FR 2d manifold $\mathbb{L}$
515	1.804745e−07, 9.509509e−07	1.994842e−05, 7.579900e−05
984	4.655299e−08, 2.420175e−07	5.777222e−06, 2.367189e−05
1963	1.189424e−08, 7.080166e−08	2.417198e−06, 1.211279e−05

Table 3 L^2, H^1 norms of the error in the Invariance Equation for the 1d unstable manifold over the $\mathbb{L}$ domain: $\epsilon_1 = -10^{-2}$, $\beta = 1$, $\alpha = 2.61$, and $\epsilon_2 = 10^{-3}$

ne	FKS 1d manifold $\mathbb{L}$
100	5.917243e−06, 3.220924e−05
200	3.034783e−06, 1.762897e−05
415	1.608347e−06, 1.365313e−05

Table 4 L^2, H^1 norms of the error in the Invariance Equation for the 1d unstable manifold over the door domain: $\epsilon_1 = -10^{-3}$, $\beta = 1$, $\alpha = 3$, and $\epsilon_2 = 10^{-4}$

ne	FKS 1d manifold Door
123	5.205366e−07, 3.332087e−06
260	2.756197e−07, 2.031136e−06
522	1.475957e−07, 1.165217e−06

Table 5 L^2, H^1 norms of the error in the Invariance Equation for the 1d unstable manifold over the polygon with holes: $\epsilon_1 = -10^{-2}$, $\beta = 1$, $\alpha = 3$, and $\epsilon_2 = 10^{-3}$

ne	FKS 1d manifold Polygon
89	4.189854e−06, 2.861762e−05
195	2.060725e−06, 2.150568e−05
391	1.126009e−06, 1.572476e−05

Table 6 L^2 norms of the error in the Invariance Equation for 1 dimensional manifolds in the Fisher model over the $\mathbb{L}$ domain with piecewise linear and Argyris basis: $\alpha = 2.7$

ne	Fisher 1d manifold piecewise linear	Fisher 1d manifold Argyris
423	6.208993e−07	5.777960e−16

we obtain defects on the order of machine precision. The later are considerably more difficult to implement, but offers significant advantages, and are especially encouraging for potential future applications in computer assisted proofs.

5 Conclusions

We have combined the parameterization method with finite element analysis to obtain a new approximation method for unstable manifolds of equilibrium solutions for parabolic PDEs. The method is applied to several PDEs defined on planar polygonal domains and is implemented for number of example problems with both polynomial and non-polynomial nonlinearities, for unstable manifolds of dimension one and two, for a number of non-convex and non-simply connected domains, and for problems involving both Laplacian and bi-harmonic Laplacian diffusion operators. The method is easy to implement for computing the approximation to arbitrary order: the same code that computes the second order approximation will compute the approximation to order 50—this is just a matter of changing a loop variable. The method is amenable to a-posteriori analysis of errors and we employ these indicators to show that our calculations are accurate far from the equilibrium solution.

Interesting future projects would be to apply the method to problems with other boundary conditions such as Dirichlet or Robin, to apply it to problems formulated on spatial domains of dimension 3 or more, to extend the method for the computation of unstable manifolds

attached to periodic solutions of parabolic PDEs, or to extend the method to study invariant manifolds attached to equilibrium or periodic solutions of systems of parabolic PDEs.

Finally we mention that there is a thriving literature on mathematically rigorous computer assisted proof for elliptic PDEs based on finite element analysis. See for example the works of [5, 37, 39–46, 49–51, 57–59] for validated numerical methods for solving nonlinear elliptic PDE (equilibrium solutions of parabolic PDEs) and their associated eigenvalue/eigenfunction problems. We refer also the references just cited for more complete review of this literature. From the point of view of the present discussion the important point is this: that the present work reduces the problem of computing jets of unstable manifolds to the problem of solving elliptic boundary value problems—and moreover that a number of authors have developed powerful methods of computer assisted proof for solving such problems. A very interesting line of future research would be to combine the results of the present work validated numerical methods for elliptic BVPs.

Acknowledgements The authors would like to thank Rafael de la Llave, Michael Plum, and Allan Hungria for helpful discussions as this work evolved. J.G. and J.D.M.J. were partially supported by the Sloan Foundation Grant FIDDS-17. J.D.M.J. was partially supported by the National Science Foundation grant DMS - 1813501.

Funding J.G. and J.D.M.J. were partially supported by the Sloan Foundation Grant FIDDS-17. J.D.M.J. was partially supported by the National Science Foundation grant DMS - 1813501.

Data Availibility Statement The data that support the findings of this study are available on request from the corresponding author J.D.M.J.

Appendix A: Formal solution of Eq. (2.5): an ODE example

In this section we illustrate the use of the parameterization method as a computational tool for a simple example. The idea is to develop a formal series solution of Eq. (2.5). Such formal calculations play a critical role in the remainder of the present work, and are much more involved for PDEs than for ODEs. To separate those complications which are inherent to the method from those which are due to PDEs, we explain the procedure for the planar vector field $F\colon \mathbb{R}^2 \to \mathbb{R}^2$ (Hilbert space is the plane) given by

$$F(x, y) = \begin{pmatrix} x + y \\ 1 - x^2 \end{pmatrix}. \tag{A.1}$$

We are interested in the orbit structure of $\mathbb{R}^2$ generated by the ODE

$$\frac{d\gamma}{dt} = F(\gamma),$$

where

$$\gamma(t) = \begin{pmatrix} x(t) \\ y(t) \end{pmatrix}.$$

Note for future use that

$$DF(x, y) = \begin{pmatrix} 1 & 1 \\ -2x & 0 \end{pmatrix}. \tag{A.2}$$

Suppose that $p_0 \in \mathbb{R}^2$ has $F(p_0) = 0$, so that p_0 is an equilibrium solution of the ODE. Suppose further that $DF(p_0)$ has one unstable eigenvalue $\lambda > 0$ and that the remaining eigenvalue is stable. Let $\xi \in \mathbb{R}^2$ denote an eigenvector associated with λ.

We look for a function $P\colon [-1,1] \to \mathbb{R}^2$ with

$$P(0) = p_0 \qquad \text{and} \qquad P'(0) = \xi,$$

parameterizing the one dimensional unstable manifold attached to p_0. In the one dimensional case the invariance equation of Equation (2.5) reduces to

$$\lambda\theta \frac{d}{d\theta} P(\theta) = F(P(\theta)), \tag{A.3}$$

for $\theta \in (-1,1)$. We look for a formal power series solution of Equation (A.3) of the form

$$P(\theta) = \begin{pmatrix} P_1(\theta) \\ P_2(\theta) \end{pmatrix} = \sum_{n=0}^{\infty} \begin{pmatrix} a_n \\ b_n \end{pmatrix} \theta^n,$$

and impose first order constraints

$$\begin{pmatrix} a_0 \\ b_0 \end{pmatrix} = p_0, \qquad \text{and} \qquad \begin{pmatrix} a_1 \\ b_1 \end{pmatrix} = \xi.$$

To work out the higher order coefficients we note that, on the level of formal power series, the left hand side of Eq. (A.3) is

$$\lambda\theta \frac{d}{d\theta} P(\theta) = \sum_{n=0}^{\infty} \lambda n \begin{pmatrix} a_n \\ b_n \end{pmatrix} \theta^n, \tag{A.4}$$

and that the right hand side of Eq. (A.3) is

$$\begin{aligned} F(P(\theta)) &= \begin{pmatrix} P_1(\theta) + P_2(\theta) \\ 1 - P_1(\theta)^2 \end{pmatrix} \\ &= \sum_{n=0}^{\infty} \begin{pmatrix} a_n + b_n \\ \delta_n - \sum_{k=0}^{n} a_{n-k} a_k \end{pmatrix} \theta^n. \end{aligned} \tag{A.5}$$

Here we have used the Cauchy product formula for the coefficients of $P_1(\theta)^2$, and defined

$$\delta_n = \begin{cases} 1 & n = 0 \\ 0 & n \geq 1 \end{cases}.$$

Returning to the invariance Eq. (A.3), we set the right hand side of Eq. (A.4) equal to Eq. (A.5), match like powers of θ, and recall the definition of δ_n to obtain

$$\lambda n \begin{pmatrix} a_n \\ b_n \end{pmatrix} = \begin{pmatrix} a_n + b_n \\ -\sum_{k=0}^{n} a_{n-k} a_k \end{pmatrix}, \tag{A.6}$$

for $n \geq 1$. We seek to isolate terms of order n, and derive a equation for p_n in terms of lower order coefficients. Since there are still some terms order n locked in the sum, we note that for $n \geq 2$

$$\sum_{k=0}^{n} a_{n-k} a_k = 2a_0 a_n + \sum_{k=1}^{n-1} a_{n-k} a_k,$$

where the new sum on the right contains no terms of order n. Exploiting this identity, Eq. (A.6) becomes

$$n\lambda \begin{pmatrix} a_n \\ b_n \end{pmatrix} = \begin{pmatrix} a_n + b_n \\ -2a_0 a_n - \sum_{k=1}^{n-1} a_{n-k} a_k \end{pmatrix},$$

or

$$\begin{pmatrix} a_n + b_n - n\lambda a_n \\ -2a_0 a_n - n\lambda b_n \end{pmatrix} = \begin{pmatrix} 0 \\ \sum_{k=1}^{n-1} a_{n-k} a_k \end{pmatrix}.$$

This is

$$\begin{bmatrix} 1 - n\lambda & 1 \\ -2a_0 & -n\lambda \end{bmatrix} \begin{pmatrix} a_n \\ b_n \end{pmatrix} = \begin{pmatrix} 0 \\ \sum_{k=1}^{n-1} a_{n-k} a_k \end{pmatrix},$$

which, after referring back to Eq. (A.2), we rewrite as

$$(DF(a_0, b_0) - n\lambda \mathrm{Id})\, p_n = s_n, \qquad n \geq 2, \tag{A.7}$$

where

$$p_n = \begin{pmatrix} a_n \\ b_n \end{pmatrix}, \qquad \text{and} \qquad s_n = \begin{pmatrix} 0 \\ \sum_{k=1}^{n-1} a_{n-k} a_k \end{pmatrix}.$$

Again, note that s_n depends only on terms of order less than n.

We refer to Eq. (A.7) as the *homological equations* for P, and note that they are linear algebraic equations for the power series coefficients of the parameterization. We now ask, *are the homological equations solvable?* To answer this we note that since $P(0) = p_0 = (a_0, b_0)$ is an equilibrium solution, the left hand side of Eq. (A.7) is the characteristic matrix for the derivative $DF(p_0)$. The characteristic matrix is invertible if and only if $n\lambda$ is not an eigenvalue of $DF(p_0)$. Since $\lambda > 0$, and since the remaining eigenvalue of $DF(p_0)$ is negative, we see that for $n \geq 2$, $n\lambda$ is never an eigenvalue. Then the homological equations are uniquely solvable to all orders, and the power series solution of Eq. (A.3), when F is given by Eq. (A.1), is well defined. Convergence of this series is another issue, not treated here.

Nevertheless, we see that the coefficients of P are uniquely determined by the first order data (equilibrium and eigenvector). Then the only freedom in determining the solution is the choice of the scaling of the eigenvector ξ. This non-uniqness is used to control the growth rate of the coefficients of P, providing numerical stability.

Remark A.1 (Non-resonance and the parameterization method) The condition

$$n\lambda \notin \mathrm{spec} DF(p_0) \qquad n \geq 2, \tag{A.8}$$

is called a non-resonance condition. In fact it is an *inner non-resonance condition* as we are computing the unstable manifold, and Eq. (A.8) involves linear combinations of the (in this case unique) unstable eigenvalues. We will see in Sect. 3 that the non-resonance conditions are similar, but somewhat more subtle for higher dimensional unstable manifolds.

Remark A.2 (Stable manifolds for ODEs) Note that replacing λ with a stable eigenvalue in the above discussion changes nothing. This reflects the general fact that in finite dimensions, the parameterization method applies equally well to both stable and unstable manifolds. However, an equilibrium solution of a parabolic PDE typically has infinitely many stable eigenvalues which make it impossible to overcome the non-resonance conditions. This is why the present work focuses on unstable manifolds for parabolic PDEs.

Appendix B: A numerical example

The vector field of Eq. (A.1) has equilibrium solutions $f(x_{1,2}, y_{1,2}) = (0, 0)$ at

$$\begin{pmatrix} x_1 \\ y_1 \end{pmatrix} = \begin{pmatrix} -1 \\ 1 \end{pmatrix}, \qquad \text{and} \qquad \begin{pmatrix} x_2 \\ y_2 \end{pmatrix} = \begin{pmatrix} 1 \\ -1 \end{pmatrix},$$

and one can check that

$$DF(-1,1) = \begin{pmatrix} 1 & 1 \\ 2 & 0 \end{pmatrix}, \tag{B.1}$$

has eigenvalues $2, -1$. Hence the equilibrium $(-1, 1)$ is a hyperbolic saddle. Let $\lambda = 2$ denote the unstable eigenvalue. One can check that

$$\xi = \begin{pmatrix} 1 \\ 1 \end{pmatrix},$$

is an associated unstable eigenvector.

The zero-th and first order terms of the parameterization are

$$\begin{pmatrix} a_0 \\ b_0 \end{pmatrix} = \begin{pmatrix} -1 \\ 1 \end{pmatrix} \quad \text{and} \quad \begin{pmatrix} a_1 \\ b_1 \end{pmatrix} = \begin{pmatrix} 1 \\ 1 \end{pmatrix},$$

and the second order term is determined by solving the homological equation of Eq. (A.7) with $n = 2$ as follows. Recalling the definition of s_n, and noting that $a_1 = 1$, when $n = 2$ we have that

$$\sum_{k=1}^{n-1} a_{n-k} a_k \Big|_{n=2} = a_1^2 = 1,$$

and that

$$s_2 = \begin{pmatrix} 0 \\ 1 \end{pmatrix}.$$

Moreover, since $\lambda = 2$ and $a_0 = -1$ we recall Eq. (B.1), and have that

$$DF(-1,1) - 2\lambda \mathrm{Id} = \begin{bmatrix} 1 - 2\lambda & 1 \\ 2 & -2\lambda \end{bmatrix} = \begin{bmatrix} -3 & 1 \\ 2 & -4 \end{bmatrix}.$$

Solving

$$[DF(-1,1) - 2\lambda \mathrm{Id}]\, p_2 = s_2,$$

gives

$$p_2 = \begin{pmatrix} -0.1 \\ -0.3 \end{pmatrix}.$$

From this we conclude that the second order local unstable manifold approximation is

$$P^N(\theta) = \begin{pmatrix} -1 \\ 1 \end{pmatrix} + \begin{pmatrix} 1 \\ 1 \end{pmatrix} \theta + \begin{pmatrix} -0.1 \\ -0.3 \end{pmatrix} \theta^2, \tag{B.2}$$

for $N = 2$. Third and higher order terms are computed recursively following the same recipe.

Roughly speaking, how accurate is the approximation above? Since the remainder term in the approximation given by P^2 in Eq. (B.2) is cubic in θ, we expect that the size of the truncation error has

$$E_2(\theta) = \|P(\theta) - P^2(\theta)\| \leq C|\theta|^3,$$

for some constant C. Suppose that we restrict the domain of our parameterization to

$$\theta \in [-10^{-5}, 10^{-5}].$$

Then E_2 is of order $(10^{-5})^3 = 10^{-15}$, so that the size of the truncation error is roughly 5 multiples machine precision. In practice, we prefer to rescale the length of the eigenvector, and take the domain of P^N normalized to a unit cube. See the following remark.

Remark B.1 *(Rescaling the eigenvector to optimizing the coefficient decay)* Suppose now that we compute the coefficients of P^N to order $N = 20$, using the same eigenvector $\xi = [1, 1]$. Rather than listing the resulting coefficients order by order, we remark that the coefficients decay like

$$\|p_n\| \approx 65 \times 10^{-1.18n},$$

(found by taking an exponential best fit algorithm) and that

$$\|p_{20}\| \approx 1.56 \times 10^{-22},$$

a quantity far smaller than machine precision. Note that coefficients below machine precision do not contribute (numerically) to the approximation, and this is wasted effort.

To obtain a more significant result, we increase the scaling of the unstable eigenvector, taking $P'(0) = s\xi$ with some $s > 1$. For example, rescaling the eigenvector by $s = 2.5$ and recomputing the coefficients leads to a 20-th order polynomial whose final coefficient vector has magnitude 1.4×10^{-14}. Since the final coefficient is close to, but still above machine

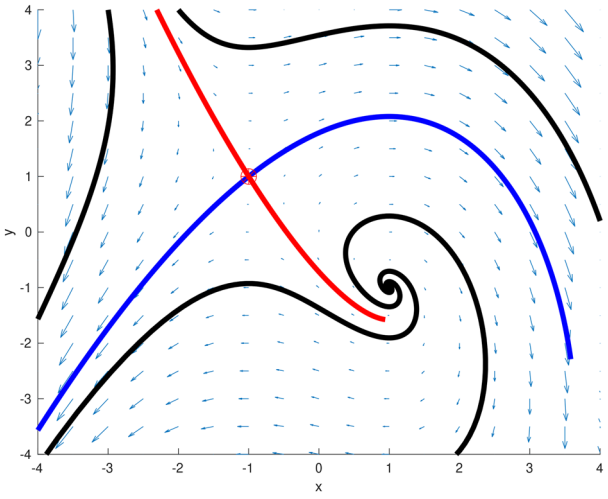

Fig. 12 Stable/unstable manifold visualization: dynamics generated by the vector field given in Eq. (A.1). Several reference orbits are illustrated by black curves. These are obtained by numerical integration of several arbitrarily chosen initial conditions. The main features of the phase space are the saddle equilibrium at $(-1, 1)$ and the repelling equilibrium at $(1, -1)$. We compute the local unstable and local stable manifold parameterizations P^N and Q^N for the saddle stable equilibrium $(-1, 1)$ to order $N = 100$. The unstable and stable eigenvectors to lengths of 13 and 10.5 respectively, The images $P^N([-1, 1])$ and $Q^N([-1, 1])$ are plotted as blue (unstable) and red (stable) curves. In both cases the plots of the manifolds are generated only by plotting the approximating polynomials: the manifolds are not extended using numerical integration. This illustrates that it is often possible to approximate a substantial portion of the unstable manifold using the parameterization method. (Of course numerical integration could be used to extend the manifolds even further). We observe that the unstable manifold parameterization (blue curve) follows a "fold", that is, the curve is not the graph over the unstable eigenspace of any function. The stable manifold on the other hand seems have been approximated up to very near it's maximal radius of convergence, as computing additional terms has very little effect on the picture, and we are not able to reach a fold

precision—and hence numerically significant—this choice of scaling is nearly optimal for the order $N = 20$ calculation.

Experimenting a little more in this way, we find that taking $s = 13$, and computing the parameterization to order $N = 100$, gives coefficients which decay exponentially fast and in such at way that the last coefficient had magnitude roughly machine epsilon. A plot illustrating the results of the order $N = 100$ calculation is given in Fig. 12. Note that the unstable manifold, which is shown as the blue curve, is not the graph of a function over the tangent space (span of the eigenvector). This illustrates the well known fact that the parameterization method can "follow folds" in the manifold. The reader interested in more refined approaches to choosing the computational parameters in the parameterization method might consult [4], where methods for optimizing the calculations under certain constraints are discussed in detail.

Remark B.2 *(Visualization in a Function space)* The parameterization method is extremely valuable for visualizing invariant manifolds when the dimension of the phase space is low. However the remainder of the paper concerns infinite dimensional problems, and visualization is much more problematic. For the parabolic PDEs studied below, the phase space is a Sobolev space, and each point on the manifold is actually a function represented as a linear combination of finite elements. In this setting it is more natural to plot the points on the manifolds as functions over the given domain. That is, we visualize the manifold as a curve or surface of functions. Nevertheless, it is valuable to keep in mind the picture in Fig. 12 when trying to interpret the results.

Appendix C: Proof of Lemma 2.1

Observe that the constraint given in Eq. (2.3) implies that P is tangent to the unstable eigenspace of $DF(u_0)$ at u_0. Since the eigenvalues are real and distinct, the eigenvectors are linearly independent, and P maps a small enough neighborhood of the origin diffeomorphically into $\mathcal{H}$.

Fix $\theta \in (-1, 1)^M$, and define the curve $\gamma_\theta : (-\infty, 0] \to \mathcal{H}$ by

$$\gamma_\theta(t) = P\left(e^{\Lambda t}\theta\right).$$

We observe that γ_θ is a solution curve for F. To see this, we first note that γ_θ is well defined for all backward time, as for all $t \in (-\infty, 0]$ we have that

$$\hat{\theta} := e^{\Lambda t}\theta \in \mathbb{B}.$$

This is because the entries of Λ are unstable, real, and distinct. To see that $\gamma_\theta(t)$ solves the differential equation, note that

$$\begin{aligned}
\frac{d}{dt}\gamma_\theta(t) &= \frac{d}{dt} P\left(e^{\Lambda t}\theta\right) \\
&= DP\left(e^{\Lambda t}\theta\right)\Lambda e^{\Lambda t}\theta \\
&= DP(\hat{\theta})\Lambda\hat{\theta} \\
&= F(P(\hat{\theta})) \\
&= F(P(e^{\Lambda t}\theta)) \\
&= F(\gamma_\theta(t)),
\end{aligned}$$

as desired.

In addition to being a solution curve, we have that γ_θ accumulates at u_0 in backward time. To see this, we simply compute the limit

$$\begin{aligned}\lim_{t\to-\infty}\gamma_\theta(t) &= \lim_{t\to-\infty} P\left(e^{\Lambda t}\theta\right)\\ &= P\left(\lim_{t\to-\infty} e^{\Lambda t}\theta\right)\\ &= P\,(0)\\ &= u_0,\end{aligned}$$

where we have used the assumption that P is smooth, and hence continuous on $[-1, 1]^M$. Since θ was arbitrary, we see that every point $P(\theta)$ on the image of P has a backward orbit which accumulates at u_0. That is

$$\text{image}(P) \subset W^u(u_0).$$

Since image(P) is locally an M-dimensional disk containing u_0 and contained in the unstable manifold, we have that image(P) is a local unstable manifold as desired.

References

1. Babuška, I., Aziz, A.K.: Survey lectures on the mathematical foundations of the finite element method. In: The Mathematical Foundations of the Finite Element Method with Applications to Partial Differential Equations (Proceedings of Symposium, University of Maryland, Baltimore, Md., 1972), Academic Press, New York, pp. 1–359. With the collaboration of G. Fix and R. B. Kellogg (1972)
2. Barker, B., Mireles James, J., Morgan, J.: Parameterization method for unstable manifolds of standing waves on the line, SIAM. J. Appl. Dyn. Syst. **19**, 1758–1797 (2020). https://doi.org/10.1137/19M128243X
3. Blair, J.J.: Higher order approximations to the boundary conditions for the finite element method. Math. Comput. **30**, 250–262 (1976) http://links.jstor.org/sici?sici=0025-5718(197604)30:134<250:HOATTB>2.0.CO;2-X&origin=MSN
4. Breden, M., Lessard, J.-P., Mireles James, J.D.: Computation of maximal local (un)stable manifold patches by the parameterization method. Indag. Math. (N.S.) **27**, 340–367 (2016). https://doi.org/10.1016/j.indag.2015.11.001
5. Breuer, B., McKenna, P.J., Plum, M.: Multiple solutions for a semilinear boundary value problem: a computational multiplicity proof. J. Differ. Equ. **195**, 243–269 (2003)
6. Breunung, T., Haller, G.: Explicit backbone curves from spectral submanifolds of forced-damped nonlinear mechanical systems. In: Proceedings of A., 474, pp. 20180083, 25 (2018). https://doi.org/10.1098/rspa.2018.0083
7. Budanur, N.B., Cvitanović, P.: Unstable manifolds of relative periodic orbits in the symmetry-reduced state space of the Kuramoto-Sivashinsky system. J. Stat. Phys. **167**, 636–655 (2017). https://doi.org/10.1007/s10955-016-1672-z
8. Budanur, N.B., Short, K.Y., Farazmand, M., Willis, A.P., Cvitanović, P.: Relative periodic orbits form the backbone of turbulent pipe flow. J. Fluid Mech. **833**, 274–301 (2017). https://doi.org/10.1017/jfm.2017.699
9. Buza, G., Jain, S., Haller, G.: Using spectral submanifolds for optimal mode selection in nonlinear model reduction. In: Proceedings of A., 477, pp. Paper No. 20200725, 21 (2021). https://doi.org/10.1098/rspa.2020.0725
10. Cabré, X., Fontich, E., de la Llave, R.: The parameterization method for invariant manifolds. I. Manifolds associated to non-resonant subspaces. Indiana Univ. Math. J. **52**, 283–328 (2003)
11. Cabré, X., Fontich, E., de la Llave, R.: The parameterization method for invariant manifolds. II. Regularity with respect to parameters. Indiana Univ. Math. J. **52**, 329–360 (2003)
12. Cabré, X., Fontich, E., de la Llave, R.: The parameterization method for invariant manifolds. III. Overview and applications. J. Differ. Equ. **218**, 444–515 (2005)
13. Cabré, X., Fontich, E., De La Llave, R.: The parameterization method for invariant manifolds iii: overview and applications. J. Differ. Equ. **218**, 444–515 (2005)

14. Christiansen, F., Cvitanović, P., Putkaradze, V.: Spatiotemporal chaos in terms of unstable recurrent patterns. Nonlinearity **10**, 55–70 (1997)
15. Ciarlet, P.G.: The finite element method for elliptic problems, North-Holland Publishing Co., Amsterdam-New York-Oxford. Studies in Mathematics and its Applications, Vol. 4 (1978)
16. Ciarlet, P.G.: The finite element method for elliptic problems, vol. 40 of classics in applied mathematics, Society for Industrial and Applied Mathematics (SIAM), Philadelphia, PA, (2002). https://doi.org/10.1137/1.9780898719208. Reprint of the 1978 original [North-Holland, Amsterdam; MR0520174 (58 #25001)]
17. de la Llave, R., Sire, Y.: An a posteriori KAM theorem for whiskered tori in Hamiltonian partial differential equations with applications to some ill-posed equations. Arch. Ration. Mech. Anal. **231**, 971–1044 (2019). https://doi.org/10.1007/s00205-018-1293-6
18. Domínguez, V., Sayas, F.-J.: Algorithm 884: a simple Matlab implementation of the Argyris element. ACM Trans. Math. Softw. 35, Art. 16, 11 (2009). https://doi.org/10.1145/1377612.1377620
19. Evans, L.C.: Partial differential equations, vol. 19 of graduate studies in mathematics, American Mathematical Society, Providence, RI, second ed. (2010). https://doi.org/10.1090/gsm/019
20. Fix, G.J., Gunzburger, M.D., Peterson, J.S.: On finite element approximations of problems having inhomogeneous essential boundary conditions. Comput. Math. Appl. **9**, 687–700 (1983). https://doi.org/10.1016/0898-1221(83)90126-8
21. Fleurantin, E., James, J.D.M.: Resonant tori, transport barriers, and chaos in a vector field with a Neimark-Sacker bifurcation. Commun. Nonlinear Sci. Numer. Simul. **85**, 105226 (2020). https://doi.org/10.1016/j.cnsns.2020.105226
22. Groothedde, C.M., Mireles James, J.D.: Parameterization method for unstable manifolds of delay differential equations. J. Comput. Dyn. **4**, 21–70 (2017). https://doi.org/10.3934/jcd.2017002
23. Halcrow, J., Gibson, J.F., Cvitanović, P., Viswanath, D.: Heteroclinic connections in plane Couette flow. J. Fluid Mech. **621**, 365–376 (2009). https://doi.org/10.1017/S0022112008005065
24. Haro, A., Canadell, M., Figueras, J.-L., Luque, A., Mondelo, J.-M.: The parameterization method for invariant manifolds, vol. 195 of applied mathematical sciences, Springer, [Cham] (2016). https://doi.org/10.1007/978-3-319-29662-3. From rigorous results to effective computations
25. Haro, À., de la Llave, R.: A parameterization method for the computation of invariant tori and their whiskers in quasi-periodic maps: numerical algorithms. Discrete Contin. Dyn. Syst. Ser. B **6**, 1261–1300 (electronic) (2006). https://doi.org/10.3934/dcdsb.2006.6.1261
26. Haro, A., de la Llave, R.: A parameterization method for the computation of invariant tori and their whiskers in quasi-periodic maps: rigorous results. J. Differ. Equ. **228**, 530–579 (2006). https://doi.org/10.1016/j.jde.2005.10.005
27. Haro, A., de la Llave, R.: A parameterization method for the computation of invariant tori and their whiskers in quasi-periodic maps: explorations and mechanisms for the breakdown of hyperbolicity. SIAM J. Appl. Dyn. Syst. **6**, 142–207 (electronic) (2007). https://doi.org/10.1137/050637327
28. He, X., de la Llave, R.: Construction of quasi-periodic solutions of state-dependent delay differential equations by the parameterization method II: Analytic case. J. Differ. Equ. **261**, 2068–2108 (2016). https://doi.org/10.1016/j.jde.2016.04.024
29. He, X., de la Llave, R.: Construction of quasi-periodic solutions of state-dependent delay differential equations by the parameterization method I: Finitely differentiable, hyperbolic case. J. Dyn. Differ. Equ. **29**, 1503–1517 (2017). https://doi.org/10.1007/s10884-016-9522-x
30. Johnson, M.E., Jolly, M.S., Kevrekidis, I.G.: The Oseberg transition: visualization of global bifurcations for the Kuramoto-Sivashinsky equation. Int. J. Bifur. Chaos Appl. Sci. Eng. **11**, 1–18 (2001). https://doi.org/10.1142/S0218127401001979
31. Jorba, À., Zou, M.: A software package for the numerical integration of ODEs by means of high-order Taylor methods. Exp. Math. **14**, 99–117 (2005). http://projecteuclid.org/getRecord?id=euclid.em/1120145574
32. Knuth, D.E.: The art of computer programming. Vol. 2, Addison-Wesley Publishing Co., Reading, Mass., second ed. Seminumerical algorithms, Addison-Wesley Series in Computer Science and Information Processing (1981)
33. Kogelbauer, F., Haller, G.: Rigorous model reduction for a damped-forced nonlinear beam model: an infinite-dimensional analysis. J. Nonlinear Sci. **28**, 1109–1150 (2018). https://doi.org/10.1007/s00332-018-9443-4
34. Kuramoto, Y., Tsuzuki, T.: Persistent propagation of concentration waves in dissipative media far from thermal equilibrium. Prog. Theor. Phys. 55 (1976)
35. Lan, Y., Cvitanović, P.: Unstable recurrent patterns in Kuramoto-Sivashinsky dynamics. Phys. Rev. E (3) **78**, 026208 (2008)

36. Lessard, J.-P., Mireles James, J., Reinhardt, C.: Computer assisted proof of transverse saddle-to-saddle connecting orbits for first order vector fields. J. Dyn. Differ. Equ. **26**, 267–313 (2014). https://doi.org/10.1007/s10884-014-9367-0
37. McKenna, P.J., Pacella, F., Plum, M., Roth, D.: A computer-assisted uniqueness proof for a semilinear elliptic boundary value problem, in Inequalities and applications, vol. 161 of Internat. Ser. Numer. Math. Birkhäuser/Springer, Basel **2012**, 31–52 (2010). https://doi.org/10.1007/978-3-0348-0249-9_3
38. Mireles James, J.D., Reinhardt, C.: Fourier-Taylor parameterization of unstable manifolds for parabolic partial differential equations: Formalism, implementation, and rigorous validation, Indagationes Mathematicae, **30**, 39–80 (2019)
39. Nakao, M.T.: A numerical approach to the proof of existence of solutions for elliptic problems, Japan. J. Appl. Math. **5**, 313–332 (1988). https://doi.org/10.1007/BF03167877
40. Nakao, M.T.: A numerical verification method for the existence of solutions for nonlinear boundary value problems. In: Contributions to Computer Arithmetic and Self-Validating NNumerical Methods (Basel, vol. 7 of IMACS Ann. Comput. Appl. Math. Baltzer, Basel **1990**, 329–339 (1989)
41. Nakao, M.T.: Computable error estimates for FEM and numerical verification of solutions for nonlinear PDEs. In: Computational and Applied Mathematics, I (Dublin, North-Holland. Amsterdam **1992**, 357–366 (1991)
42. Nakao, M.T.: A numerical verification method for the existence of weak solutions for nonlinear boundary value problems. J. Math. Anal. Appl. **164**, 489–507 (1992). https://doi.org/10.1016/0022-247X(92)90129-2
43. Nakao, M.T., Hashimoto, K.: Guaranteed error bounds for finite element approximations of noncoercive elliptic problems and their applications. J. Comput. Appl. Math. **218**, 106–115 (2008)
44. Nakao, M.T., Hashimoto, K., Kobayashi, K.: Verified numerical computation of solutions for the stationary Navier-Stokes equation in nonconvex polygonal domains. Hokkaido Math. J. **36**, 777–799 (2007)
45. Nakao, M.T., Watanabe, Y.: On computational proofs of the existence of solutions to nonlinear parabolic problems. In: Proceedings of the Fifth International Congress on Computational and Applied Mathematics (Leuven, 1992) **50**, 401–410 (1994). https://doi.org/10.1016/0377-0427(94)90316-6
46. Nakao, M.T., Watanabe, Y.: An efficient approach to the numerical verification for solutions of elliptic differential equations. Numer. Algor. **37**, 311–323 (2004)
47. Nicolaenko, B., Scheurer, B., Temam, R.: Some global dynamical properties of the Kuramoto-Sivashinsky equations: nonlinear stability and attractors. Phys. D **16**, 155–183 (1985). https://doi.org/10.1016/0167-2789(85)90056-9
48. Opreni, A., Vizzaccaro, A., Boni, N., Carminati, R., Mendicino, G., Touzé, C., Frangi, A.: Fast and accurate predictions of mems micromirrors nonlinear dynamic response using direct computation of invariant manifolds. In: 2022 IEEE 35th International Conference on Micro Electro Mechanical Systems Conference (MEMS), IEEE, pp. 491–494 (2022)
49. Pacella, F., Plum, M., Rütters, D.: A computer-assisted existence proof for Emden's equation on an unbounded L-shaped domain. Commun. Contemp. Math. **19**, 1750005 (2017). https://doi.org/10.1142/S0219199717500055
50. Plum, M.: Existence and enclosure results for continua of solutions of parameter-dependent nonlinear boundary value problems. J. Comput. Appl. Math. **60**, 187–200. Linear/nonlinear iterative methods and verification of solution (Matsuyama, 1993) (1995)
51. Plum, M.: Existence and multiplicity proofs for semilinear elliptic boundary value problems by computer assistance. Jahresber. Deutsch. Math.-Verein. **110**, 19–54 (2008)
52. Scott, R.: Interpolated boundary conditions in the finite element method. SIAM J. Numer. Anal. **12**, 404–427 (1975). https://doi.org/10.1137/0712032
53. van den Berg, J.B., Mireles James, D., Lessard, J.J.-P., Mischaikow, K.: Rigorous numerics for symmetric connecting orbits: even homoclinics of the Gray-Scott equation. SIAM J. Math. Anal. **43**, 1557–1594 (2011). https://doi.org/10.1137/100812008
54. van den Berg, J.B., Mireles James, J.D.: Parameterization of slow-stable manifolds and their invariant vector bundles: theory and numerical implementation. Discrete Contin. Dyn. Syst. **36**, 4637–4664 (2016). https://doi.org/10.3934/dcds.2016002
55. van den Berg, J.B., Mireles James, J.D., Reinhardt, C.: Computing (un)stable manifolds with validated error bounds: non-resonant and resonant spectra. J. Nonlinear Sci. **26**, 1055–1095 (2016). https://doi.org/10.1007/s00332-016-9298-5
56. Vizzaccaro, A., Opreni, A., Salles, L., Frangi, A., Touzé, C.: High order direct parametrisation of invariant manifolds for model order reduction of finite element structures: application to large amplitude vibrations and uncovering of a folding point. arXiv:2109.10031 (2021)

57. Watanabe, Y., Nagatou, K., Plum, M., Nakao, M.T.: Verified computations of eigenvalue exclosures for eigenvalue problems in Hilbert spaces. SIAM J. Numer. Anal. **52**, 975–992 (2014). https://doi.org/10.1137/120894683
58. Watanabe, Y., Plum, M., Nakao, M.T.: A computer-assisted instability proof for the Orr-Sommerfeld problem with Poiseuille flow. ZAMM Z. Angew. Math. Mech. **89**, 5–18 (2009). https://doi.org/10.1002/zamm.200700158
59. Yamamoto, N., Nakao, M.T.: Numerical verifications for solutions to elliptic equations using residual iterations with a higher order finite element. J. Comput. Appl. Math. **60**, 271–279 (1995)
60. Zgliczyński, P.: Steady state bifurcations for the Kuramoto-Sivashinsky equation: a computer assisted proof. J. Comput. Dyn. **2**, 95–142 (2015). https://doi.org/10.3934/jcd.2015.2.95